

---

# DID I FAITHFULLY SAY WHAT I THOUGHT? BRIDGING THE GAP BETWEEN LLMs NEURAL ACTIVITY AND SELF-EXPLANATIONS

---

A PREPRINT

**Milan Bhan**  
Ekimetrics  
Sorbonne Université  
LIP6

**Jean-Noël Vittaut**  
Sorbonne Université  
LIP6

**Nicolas Chesneau**  
Ekimetrics

**Sarath Chandar**  
Mila  
Chandar Research Lab  
Polytechnique Montréal  
Canada CIFAR AI Chair

**Marie-Jeanne Lesot**  
Sorbonne Université  
LIP6

October 6, 2025

## ABSTRACT

Large Language Models (LLMs) can generate plausible free text self-explanations to justify their answers. However, these natural language explanations may not accurately reflect the model’s actual reasoning process, indicating a lack of faithfulness. Existing faithfulness evaluation methods rely primarily on behavioral tests or computational block analysis without examining the semantic content of internal neural representations. This paper proposes *NeuroFaith*, a flexible framework that measures the faithfulness of LLM free text self-explanation by identifying key concepts within explanations and mechanistically testing whether these concepts actually influence the model’s predictions. We show the versatility of *NeuroFaith* across 2-hop reasoning and classification tasks. Additionally, a linear faithfulness probe based on *NeuroFaith* is developed to detect unfaithful self-explanations from representation space and improve faithfulness through steering. *NeuroFaith* provides a principled approach to evaluating and enhancing the faithfulness of LLM free text self-explanations, addressing critical needs for trustworthy AI systems.

## 1 Introduction

Autoregressive Large Language Models (LLMs) can generate plausible self Natural Language Explanation (self-NLE) to support their answers (Wiegrefe & Marasovic; Huang et al., 2023). Generating self-NLE consists of prompting the LLM to generate an explanation in a *predict-then-explain* setting, where the model first generates a response to a question and then produces a self-NLE as a justification. Unlike their non-generative predecessors, modern LLMs are trained to generate both answers and free text self-NLE that appear credible despite potentially containing persuasive hallucinations (Sahoo et al., 2024). This way, despite their logical and coherent appearance favoring trust in the model (Han et al., 2023), LLM-generated self-NLE turn out to not systematically reflect the actual underlying decision-making process of the model, creating a tension between self-NLE *plausibility* and *faithfulness* (Agarwal et al., 2024).

Faithfulness, as defined by Jacovi & Goldberg (2020), measures “how accurately the explanation reflects the true reasoning process of the model”, a definition widely adopted in the literature (Lyu et al., 2024) and which we likewise follow throughout this work. Unfaithful self-NLE can have serious consequences in critical domains, where explanations that appear plausible but lack faithfulness might lead end-users to over-rely on model predictions and make

unfair (Luo et al., 2022) or harmful (Kayser et al., 2024) decisions. As the use of LLMs is expanding across diverse fields, the combination of their widespread adoption and the simplicity of generating self-NLE through prompting make evaluating their faithfulness increasingly critical.

Assessing self-NLE faithfulness presents profound difficulties. Unlike more structured explainability methods such as attribution (Wiegrefe et al., 2021) or counterfactual approaches (Madsen et al., 2024), the free-form nature of natural language explanations makes faithfulness evaluation particularly difficult. Numerous methods have been developed to measure self-explanation faithfulness (see e.g. Lyu et al. (2024)). However, (1) they mostly perform behavioral tests and do not examine LLM internal reasoning processes (Atanasova et al., 2023; Siegel et al., 2024, 2025; Matton et al., 2025), and (2) they identify the computational blocks that contribute to prediction and self-NLE without conducting semantic analysis of the neural representations within these blocks (Wiegrefe et al., 2021; Parcalabescu & Frank, 2024; Yeo et al., 2024). These shortcomings have led these methods to be characterized as measuring *self-consistency* rather than genuine faithfulness (Parcalabescu & Frank, 2024), since they fail to establish direct connections between explanations and the model’s actual reasoning processes. To overcome these limitations, we introduce **NeuroFaith**, a flexible framework for directly measuring LLM self-explanation faithfulness. Our main contributions are as follows:

1. **NeuroFaith** measures the alignment between LLM internal reasoning and its self-explanations by identifying key concepts within the explanation and mechanistically testing whether these concepts actually influence the model’s predictions.
2. We demonstrate the versatility of **NeuroFaith** by applying it to both 2-hop reasoning tasks and classification problems.
3. We develop a linear faithfulness probe based on **NeuroFaith** to efficiently detect unfaithful LLM self-explanations from representation space and improve faithfulness through steering.

This paper is organized as follows: Section 2 presents how existing approaches measure the faithfulness of LLM self-NLE. Section 3 introduces the **NeuroFaith** framework. In Sections 4 and 5, we instantiate **NeuroFaith** for two different tasks, 2-hop reasoning and classification respectively. We finally show in Section 6 that self-NLE faithfulness, as measured by **NeuroFaith**, can be linearly detected in LLM representation space and improved through steering.

## 2 Related Work

Numerous approaches have been proposed to measure self-NLE faithfulness (Lyu et al., 2024). One approach (Tutek et al., 2025) assesses the effect of unlearning (Liu et al., 2025) the parametric knowledge encoded in the reasoning steps of the self-NLE. The higher the change in prediction between the original model and the model having unlearned the reasoning steps, the more faithful the self-NLE. We group the remaining approaches in two categories.

**Counterfactual Interventions.** NLE faithfulness can be assessed through behavioral tests that measure how perturbations in the input text affect both predictions and self-NLE (Atanasova et al., 2023). Counterfactual Intervention (CI) methods employ auxiliary models to generate counterfactual texts designed to change the LLM outcome. The LLM is then prompted to produce a self-NLE to justify its new prediction. The self-NLE is deemed faithful if it aligns with the specific CI that caused the prediction change. These CI approaches mostly differ in two ways: how they measure consistency between the intervention and the resulting self-NLE (Atanasova et al., 2023; Siegel et al., 2024, 2025), and the granularity of the CI intervention (Matton et al., 2025). These approaches face several limitations: (1) the CI may not be solely responsible for the change in prediction, as the model might base its new prediction on another part of the input text after intervention, (2) CI methods treat the model as a black box by only examining input-output relationships without analyzing the internal neural processes that generate predictions, which departs from the commonly adopted definition of explanation faithfulness.

**Attribution Agreement.** Another way to measure self-NLE faithfulness is to compute post-hoc Attribution Agreement (AA) between the prediction and the NLE (Parcalabescu & Frank, 2024; Wiegrefe et al., 2021; Yeo et al., 2024). AA methods compute attribution scores for both the model’s predictions and its self-NLE and then measure the correlation between these scores to assess faithfulness. Higher correlation values indicate greater faithfulness in the model’s self-NLE. AA approaches vary in the post-hoc attribution method employed (gradient-based (Sundararajan et al., 2017), SHAP (Lundberg & Lee, 2017) or activation patching (Meng et al., 2022)). While AA methods assess whether the same LLM computational blocks were used when generating both the prediction and the self-NLE, they overlook the semantic content of neural representations, leaving the model’s reasoning process only partially treated.

In the following, we propose a framework that directly examines the correspondence between self-NLE and the model’s actual reasoning process by conducting concept-level mechanistic analysis of internal hidden states during the forward pass that generates the prediction.

### 3 NeuroFaith: A Framework for Measuring the Faithfulness of LLM self-NLE

This section introduces the core principles of NeuroFaith, our proposed flexible framework for measuring the faithfulness of LLM self-natural language explanations (self-NLE). Based on the premise that faithful explanations should accurately reflect the model’s internal reasoning process, NeuroFaith quantifies how well a self-NLE aligns with the model’s internal reasoning processes by extracting concepts from self-NLE and mechanistically evaluating their importance for the model prediction. Sections 4 and 5 provide detailed instantiations of how to apply NeuroFaith to 2-hop reasoning and classification tasks respectively. In the following, we denote an  $L$ -layer auto-regressive Transformer-based LLM  $f$ , a set of input texts  $\mathbf{X}$  and a text of interest  $x \in \mathbf{X}$ . We denote  $f(x)$  as the model’s answer and  $e(x)$  as the corresponding self-NLE produced by  $f$  for input  $x$ . NeuroFaith is a 3-step framework illustrated in Figure 1, summarized below and detailed in the next subsections.

1. **Concept Extraction.** We extract from  $e(x)$  a set of concepts  $\{c_i\}_{i=1}^P$  that influence  $f(x)$ .
2. **Concept-wise Mechanistic Interpretation.** For each concept  $c_i$ , we generate a post-hoc interpretation  $I_\Gamma(c_i)$  based on a relevant subpart of the model called circuit  $\Gamma$  and a mechanistic interpretability method called interpreter  $I$  to assess its impact on  $f(x)$ .
3. **Faithfulness Measurement.** We compute faithfulness  $F(x, e)$  by validating that the concepts  $\{c_i\}_{i=1}^P$  emphasized in the self-NLE actually have significant mechanistic effects on  $f(x)$  as determined by their interpretations  $\{I_\Gamma(c_i)\}_{i=1}^P$ .

#### 3.1 Concept Extraction

Given an input text  $x$ , a prediction  $f(x)$  and its self-NLE  $e(x)$ , the first step involves parsing the self-NLE to extract a set of concepts  $\{c_i\}_{i=1}^P$  that influence  $f(x)$ .

**Concept Definition.** Recent research has shown that interpretable binary high-level features, referred to as *concepts*, appear to be linearly encoded within LLM representation space (Elhage et al., 2022; Park et al., 2024). This computational understanding aligns with definitions from cognitive science (Ruiz Luyten & van der Schaar, 2024), where concepts are considered as mental entities essential to thought, enabling information integration and categorization (Goguen, 2005). This alignment makes concepts an ideal granularity level for model interpretation. For example in Figure 1, the concept “*Ingmar Bergman*” directly influences the prediction “*Sweden*” because Ingmar Bergman is Swedish and directed the movie *Persona*.

**Concept Extraction.** Concepts can be extracted either through human investigation or using an auxiliary LLM under LLM-as-a-Judge settings (Gu et al., 2024). Human annotation enables targeted analysis of specific concepts that are hypothesized to be important for the model’s reasoning. Human annotation provides high-quality, domain-expert identification of relevant influential concepts but is costly and may not scale to large datasets. LLM-as-a-Judge approaches offer scalability but may introduce systematic biases or miss relevant concepts that human experts would identify. We provide detailed examples of prompts used to extract concepts from self-NLE with an auxiliary LLM in Appendix D.1.

#### 3.2 Concept-wise Mechanistic Interpretation

The second step evaluates whether the concepts  $\{c_i\}_{i=1}^P$  are actually important for the model’s internal processing. We compute an attribution score  $I_\Gamma(c)$  for each concept  $c \in \{c_i\}_{i=1}^P$  using an interpretability method (interpreter  $I$ ) applied to model hidden states within a relevant subpart of the model (circuit  $\Gamma$ ). We assume each concept can be detected in the model representation space.

**Circuit.** Rather than examining every network component, we focus our mechanistic analysis on computational subgraphs that most significantly influence  $f$  prediction named *circuits* (Elhage et al., 2021). Circuits are sparse oriented subgraphs with interpretable functional roles, where nodes represent computational units and edges represent computation paths (Räuber et al., 2023). Formally, we define a circuit as  $\Gamma = (\{(k, \ell)\}, \mathcal{G})$  where  $\{(k, \ell)\}$  specifies coordinate pairs (token index, layer) for information flow in  $f$ , and  $\mathcal{G}$  defines the granularity of each computational node. The granularity  $\mathcal{G}$  represents transformer sublayers: residual stream output (RS), multi-head attention (MHA), or multi-layer perceptron (MLP) (Rai et al., 2024). This granularity avoids focusing on individual neurons due to their polysemanticity (Elhage et al., 2022). For example in Figure 1, the circuit is highlighted in blue, starting at token index

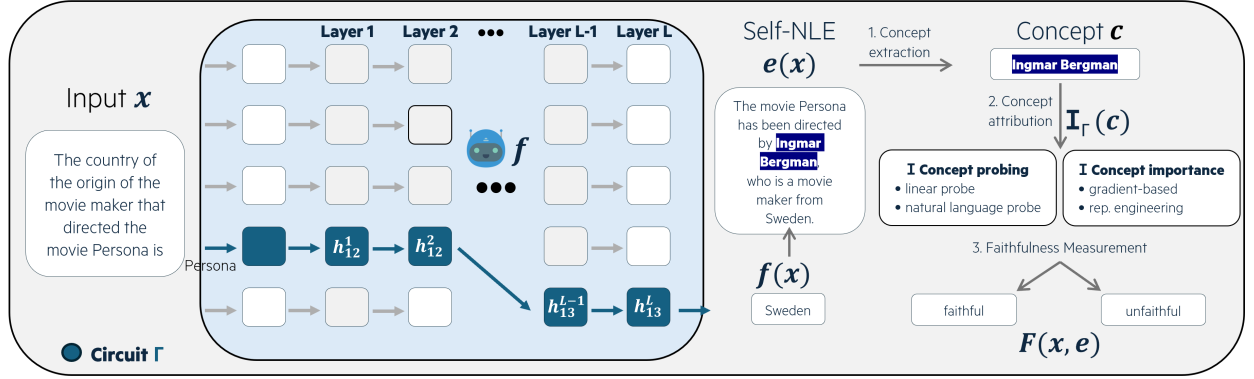


Figure 1: NeuroFaith overview. NeuroFaith (1) extracting concepts from the self-NLE and (2) assessing the mechanistic influence of these concepts to finally (3) measure faithfulness.

12 and layer 1 and finishes at token index 13 and layer L-1. Circuits can be obtained through manual investigation of task-specific patterns (Bereska & Gavves, 2024; Wang et al., 2023; Biran et al., 2024) or automated discovery via activation patching (Meng et al., 2022; Conmy et al., 2023), backward attribution (Ferrando & Voita, 2024), or Transcoders (Dunefsky et al., 2024). Additional details about circuits are in Appendix D.2.

**Mechanistic Interpreter.** To mechanistically interpret a concept  $c$  across circuit  $\Gamma$ , we use an interpreter  $I$  to compute an attribution score  $I_\Gamma(c)$  that evaluates whether  $c$  impacts  $f(x)$ . NeuroFaith implements two approaches, each suited to different objectives. **Probing** methods determine whether  $c$  is represented within  $f$  hidden states on  $\Gamma$ . This involves either generating natural language interpretations of hidden states (using Selfie (Chen et al., 2024) or Patchscopes (Ghandeharioun et al., 2024)) to detect  $c$ , or training linear probes (Belinkov, 2022) when  $c$  is linearly separable with sufficient labels to train the probe. Denoting  $h_k^\ell$  the hidden state at token  $k$  and layer  $\ell$ , we define  $I_\Gamma(c) = \max_{(k,\ell) \in \Gamma} I(h_k^\ell)$ , assessing  $c$  as important if detected in at least one hidden state from  $\Gamma$ . **Concept importance** methods approximate the causal influence of  $c$  on  $f(x)$  (Geiger et al., 2025). They use gradient-based methods like TCAV (Kim et al., 2018) or Representation Engineering (Zou et al., 2023) to directly manipulate concept-related activations across  $\Gamma$  and measure behavioral changes, providing causal evidence for concept importance. Section 5 details this procedure for measuring faithfulness in the case of classification.

### 3.3 Faithfulness Measurement

We consider the self-NLE  $e(x)$  as faithful when the extracted concepts  $\{c_i\}_{i=1}^p$  are demonstrably important for  $f$ 's internal processing according to  $I_\Gamma(c)$ . We propose to define the faithfulness of  $e(x)$  as the proportion of concepts it contains that are mechanistically assessed as important, i.e. that have a positive attribution score:  $F(x, e) = \frac{1}{p} \sum_{i=1}^p \mathbf{1}_{I_\Gamma(c_i) > 0}$ .

The faithfulness score has different meanings depending on the chosen interpreter  $I$ : **Probing-based faithfulness** measures the detection rate of explanation concepts within the model's internal representations along circuit  $\Gamma$ . High probing-based faithfulness indicate that most mentioned concepts are properly decoded from the model's hidden states. **Importance-based faithfulness** estimate causal relevance of explanation concepts for the prediction  $f(x)$ . High importance-based faithfulness indicate that most mentioned concepts actually influence  $f$  reasoning process. This framework directly captures concept-level alignment between the self-NLE  $e(x)$  and  $f$  internal reasoning process. NeuroFaith faithfulness scores either indicate that the self-NLE accurately reflects internal processing or that the explanation mentions concepts that are not mechanistically important. This way, NeuroFaith directly aligns with the established definition of explanation faithfulness introduced above (Jacovi & Goldberg, 2020), offering a principled evaluation of self-NLE faithfulness.

## 4 The Case of 2-Hop Reasoning

In the previous section, we defined the high level core principle of NeuroFaith. We now instantiate NeuroFaith to 2-hop reasoning using probing-based faithfulness, and precisely characterize self-NLE with respect to both its faithfulness and its correctness.

#### 4.1 NeuroFaith Instantiation for 2-Hop Reasoning

**Task Description.** Multi-hop reasoning is a complex cognitive task that requires connecting a sequence of objects to reach a conclusion (Mavi et al., 2024). It consists of several single-hop operations (Trivedi et al., 2022), which can individually be defined as triplets  $(o_i, r, o_j)$  where  $o_i$  is a source object,  $r$  is a relation and  $o_j$  is a target object. For example, the 2-hop reasoning statement "The country of origin of the movie maker that directed the movie *Persona* is Sweden" requires sequentially solving the two single-hop operations:  $(o_1 = \text{persona}, r_1 = \text{movie direction}, o_2 = \text{ingmar bergman})$  and  $(o_2 = \text{ingmar bergman}, r_2 = \text{country}, o_3 = \text{sweden})$ . An input text  $x$  that requires performing 2-hop reasoning can be expressed as  $x = (o_1, r_1, \blacktriangle, r_2, \bullet)$ , where  $\blacktriangle$  and  $\bullet$  are placeholders that have to be associated with respectively a bridge object ( $\widehat{o}_2$ ) and the final object answer ( $f(x) = \widehat{o}_3$ ).

**Concept Extraction.** Following the notations introduced in Section 3, given an input text  $x \in \mathbf{X}$ , if  $\widehat{o}_3 = o_3$ , the final answer is correct. Two reasoning chains are derived from  $e(x)$ :  $(o_1, r_1, \widehat{o}_2)$  and  $(\widehat{o}_2, r_2, \widehat{o}_3)$ . In this instantiation, we do concept extraction from  $e(x)$  by prompting an auxiliary LLM to get the bridge object ( $\widehat{o}_2$ ) based on  $o_1$  and  $r_1$ . This way,  $\widehat{o}_2$  is our concept  $c$  of interest, representing the critical intermediate step that connects the two reasoning operations. The next step consists in computing a post-hoc mechanistic interpretation to assess  $c$  impact on the prediction.

**Probing-based Concept Interpretation.** The presence of a single bridge object in 2-hop reasoning self-NLE makes probing-based interpretations particularly appropriate. For  $f$  to correctly answer, it must internally compute the bridge object during the first hop before executing the second hop. Therefore, detecting the extracted bridge object  $\widehat{o}_2 = c$  in  $f$  internal representations is a strong indication to assess whether  $c$  is important for the prediction. We employ natural language interpretation methods such as `Selfie` and `Patchscopes`, rather than linear probes, as they provide higher accuracy and are unsupervised (Ghandeharioun et al., 2024). Recent work (Biran et al., 2024; Yang et al., 2024) has shown that the bridge object of 2-hop reasoning was resolved on early layers and can be detected by focusing on the last token corresponding to source object  $o_1$  and the residual stream (RS). We leverage this information to define circuit  $\Gamma$  and generate the natural language description  $\tilde{h}_k^\ell$  of hidden state  $h_k^\ell$ . For concept (bridge object)  $c$ , the probing-based concept attribution is defined as  $\mathbb{I}_\Gamma(c) = 1$  iff  $\exists(k, \ell) \in \Gamma$  such that  $c \in \tilde{h}_k^\ell$ .

**Self-NLE and Latent Reasoning Characterization.** Following the notations introduced in Section 3.3,  $e(x)$  is assessed faithful if  $c$  is detected in at least one hidden state within  $\Gamma$  with the probe  $\mathbb{I}$  ( $\mathbb{I}_\Gamma(c)=1$ ). Beyond faithfulness, we can use the ground truth object ( $o_2$ ) to characterize the correctness of  $e(x)$  and the latent first hop respectively:  $e(x)$  is said to be correct (**self-NLE correctness**) if its corresponding bridge object is the expected ground truth ( $c = o_2$ ). Likewise, the model performs correct first-hop latent reasoning (**latent hop 1 correctness**) if  $\exists(k, l) \in \Gamma$  such that  $o_2 \in \tilde{h}_k^l$ . This multi-dimensional analysis provides comprehensive characterization of explanation quality and internal reasoning alignment. We give a thorough taxonomy of self-NLE in the case of 2-hop reasoning in Appendix E, based on prediction correctness, self-NLE faithfulness and correctness and latent reasoning correctness. We also propose an experimental protocol to evaluate the relevance of our faithfulness measure in Appendix F and compare NeuroFaith to CI, showing our faithfulness measure relevancy in absolute and in comparison to CI.

#### 4.2 2-Hop Reasoning Experimental Analysis

**Experimental Setup.** We evaluate NeuroFaith for 2-hop reasoning on the Wikidata-2-hop dataset (Biran et al., 2024). We apply NeuroFaith to Gemma-2-2B, Gemma-2-9B and Gemma-2-27B (Riviere et al., 2024). We use Qwen3-32B as auxiliary model to extract bridge objects from self-NLE and use the prompt from Ghandeharioun et al. (2024) to apply Patchscopes as interpreter. We evaluate **Latent Reasoning Hop 1 Correctness**, **Self-NLE Faithfulness** and **Self-NLE Correctness** based on the characterization introduced above. The results are computed according to the status of the prediction preceding the self-NLE (accurate vs. inaccurate). We give more details about the layers used to define  $\Gamma$  and the prompt used to extract the bridge object and compute the interpretations in Appendix D.1 and D.2.

**Key Findings.** Table 1 shows the aggregated experimental results obtained by applying NeuroFaith on Wikidata-2-hop. All the analyzed metrics are higher on average for accurate predictions and improve with model size. These results support that correct reasoning tend to produce more faithful and correct self-NLE. Key failure patterns emerge: approximately 45% of inaccurate predictions correctly resolve the first hop operation, indicating that failure often occurs in the second reasoning step ( $o_2, r_2, o_3$ ). This suggests that models can identify correct bridge objects even when failing to complete the full reasoning chain. The difference between latent reasoning hop 1 correctness and self-NLE correctness shows that models sometimes identify correct bridge objects internally but fail to express them in their

Model	Task Acc.	Self-NLE Correctness		Latent Hop 1 Correctness		Self-NLE Faithfulness	
		Accurate	Inaccurate	Accurate	Inaccurate	Accurate	Inaccurate
gemma-2-2b	7.1%	58.0%	56.0%	48.3%	47.4%	48.4%	57.6%
gemma-2-9b	16.6%	74.0%	55.4%	58.5%	44.3%	60.8%	55.0%
gemma-2-27b	22.3%	77.8%	55.6%	64.9%	46.9%	68.8%	60.2%

Table 1: 2-hop reasoning accuracy, first hop latent reasoning correctness and self-NLE correctness and faithfulness across models obtained from NeuroFaith. "(In)accurate" represents the set of predictions initially (in)correct.

self-NLE. This gap decreases with model size, suggesting better alignment between internal and explicit reasoning in larger models.

Remarkably, even when models produce correct final answers, they identify the correct bridge object in their internal representations only *48-65% of the time*. This suggests that models can arrive at correct answers through alternative reasoning pathways that bypass explicit bridge object computation. The models may be leveraging (1) direct associations between source and target entities (shortcut learning (Geirhos et al., 2020)), or (2) alternative pathways making the model accurately answer for a reason different than the ground truth bridge object (see category 9 in Figure 25). This phenomenon highlights that *task accuracy alone is insufficient for evaluating reasoning quality*.

## 5 The Case of Classification

This section instantiates NeuroFaith for classification problems by employing concept importance methods as the mechanistic interpreter I. For classification tasks, given an input text  $x \in \mathbf{X}$ , we denote  $f(x) = \hat{y} \in \mathcal{Y}$  with probability score  $p_{\hat{y}}(x)$  where  $\mathcal{Y}$  is the label space. We assume access to a predefined set of task-relevant concepts  $\mathcal{C}$  with concept labels for input texts.

### 5.1 NeuroFaith Instantiation for Classification

**Concept Extraction.** To enable mechanistic interpretation of each concept  $c \in \mathcal{C}$ , we compute Concept Activation Vectors (CAVs) that represent concepts as directions in  $f$  representation space. Following established practices in concept-based interpretability, we employ the mean difference (`diff-mean`) (Rimsky et al., 2024) approach for CAV computation due to its optimal balance between concept detection accuracy and computational efficiency (Wu et al., 2025). For a concept  $c \in \mathcal{C}$ , a token index  $k$  and a layer  $\ell$ , the layer-wise CAV is defined as:  $\vec{c}_\ell = \frac{1}{|\mathbf{X}_c^+|} \sum_{x \in \mathbf{X}_c^+} h_k^\ell - \frac{1}{|\mathbf{X}_c^-|} \sum_{x \in \mathbf{X}_c^-} h_k^\ell$ , where  $\mathbf{X}_c^+$  and  $\mathbf{X}_c^-$  respectively represent the sets of texts from  $\mathbf{X}$  where the concept  $c$  is present or absent and  $h_k^\ell$  denotes the hidden state at layer  $\ell$  and token position  $k$  at the specified granularity  $\mathcal{G}$ . We set the token index to the final position of  $x$ , as this location represents the model’s complete computational state prior to next-token generation. These CAVs allow for computing the importance of each concept using Representation Engineering techniques. Following Section 3, we use an auxiliary LLM to extract a set of concepts from  $e(x)$ , making sure that  $\{c_i\}_{i=1}^p \subset \mathcal{C}$ .

**Importance-based Concept Interpretation.** For a concept  $c \in \{c_i\}_{i=1}^p$ , we approximate its causal influence on  $f(x)$  through representation engineering and concept erasure (Belrose et al., 2023). We perform controlled interventions by erasing  $c$  from hidden states during forward propagation:  $h_k^\ell \leftarrow h_k^\ell - \lambda \times \vec{c}_\ell$ , where  $\lambda \in [0, 1]$  represents intervention intensity and with  $\lambda = 1$  represents maximum intervention intensity to avoid  $f$  collapse (Rimsky et al., 2024). This approach provides strong causal evidence for concept importance without requiring computationally costly gradient computations such as TCAV. We define  $\Gamma$  with granularity  $\mathcal{G}$  set to residual stream (RS), token index as the final position (likewise CAVs), and layers are selected based on concept detectability (F1 score  $> 60\%$  using layer-wise linear probes with `diff-mean`). Applying this intervention across circuit  $\Gamma$ , we measure the resulting probability score:  $p_{\hat{y}}(x, \{\text{do}(H_k^\ell = h_k^\ell - \lambda \times \vec{c}_\ell)\}_{(k,\ell) \in \Gamma})$ , where the  $\text{do}(X = x)$  operator (Pearl, 2009) represents an intervention that sets variable  $X$  to value  $x$ . We model this relationship as linear:  $p_{\hat{y}}(\cdot) = \beta_0 + \beta_1 \times \lambda$ , where the concept importance score is  $\text{I}_\Gamma(c) = \beta_1$  (i.e. the marginal effect of intervention on prediction probability, computed via linear regression across different  $\lambda$  values).  $\text{I}_\Gamma(c)$  is set to 0 when its significance  $t$ -test shows  $p > 0.01$ . This process is repeated for each extracted concept from  $e(x)$  to derive faithfulness scores as described in Section 3.3. Implementation details and examples are provided in Appendix D.2 and G.

Model	Task Acc.		Self-NLE Faithfulness			
	AGNews	Ledgar	AGNews		Ledgar	
			Accurate	Inaccurate	Accurate	Inaccurate
gemma-2-2B	86.5%	40.3%	54.6%	65.1%	58.9%	40.5%
gemma-2-9B	88.7%	59.7%	96.0%	92.3%	56.0%	58.3%
gemma-2-27B	88.9%	58.1%	74.0%	72.4%	53.0%	31.6%

Table 2: Classification accuracy and self-NLE faithfulness across models and datasets obtained from NeuroFaith. "(In)accurate represents the set of predictions initially (in)correct.

## 5.2 Classification Experimental Analysis

**Experimental Setup.** We evaluate NeuroFaith’s classification instantiation on two datasets with varying complexity: AGNews (Gulli, 2005), a newspaper article classification and Ledgar (Tugener et al., 2020), a more challenging critical domain legal document classification dataset. We apply NeuroFaith to Gemma-2-2B, Gemma-2-9B and Gemma-2-27B (Riviere et al., 2024). We use the concept set  $\mathcal{C}$  and labels of AGNews and Ledgar from Bhan et al. (2025) to compute the CAVs. We use Qwen3-32B to extract concepts from the self-NLE, ensuring extracted concepts belong to  $\mathcal{C}$  for each dataset. We focus on instances solely containing concepts that are linearly detectable in at least one layer. We evaluate **Self-NLE Faithfulness** according to the status of the prediction preceding the self-NLE (accurate vs. inaccurate).

**Key Findings.** Table 2 shows experimental results for AGNews and Ledgar datasets. Self-NLE faithfulness is consistently higher on the simpler AGNews dataset, aligning with the intuition that explanation faithfulness might decrease with task complexity. Accurate predictions generally yield more faithful explanations, suggesting that correct predictions might rely on relevant concepts. Notably, gemma-2-9B achieves the highest faithfulness scores across both datasets, indicating better alignment and going against the idea of a monotonic relationship between model scale and explanation faithfulness.

Comparing findings across classification and 2-hop reasoning reveals both general patterns and task-specific differences. *General findings:* (1) accurate predictions tend to produce more faithful explanations, and (2) increased task difficulty seems to reduce self-NLE faithfulness. However, *scaling effects vary between tasks*, indicating that the model scale-faithfulness relationship is highly task-dependent, a finding consistent with prior work (Madsen et al., 2024; Atanasova et al., 2023; Parcalabescu & Frank, 2024; Matton et al., 2025).

## 6 Linearly Detecting and Improving Self-NLE Faithfulness

Recent work has demonstrated that various AI safety behaviors naturally associated with faithfulness are encoded as linear directions in LLM representation spaces (Bereska & Gavves, 2024), such as hallucination (Rimsky et al., 2024) or deceptiveness (Goldowsky-Dill et al., 2025). We investigate whether NeuroFaith-based faithfulness exhibits linear structure enabling (1) accurate detection in representation space and (2) manipulation to improve faithfulness through activation steering.

### 6.1 Linear Detection of Faithfulness

**Faithfulness Linear Representation Computation.** We construct datasets of faithful and unfaithful self-NLE pairs using NeuroFaith scores. Unlike 2-hop reasoning tasks, classification self-NLE faithfulness yields continuous scores between 0 and 1. To ensure clear class separation, we focus on polarized cases where  $F(x) \in \{0, 1\}$  for clear separation. We construct input sequences as  $x_{nle} = [x, \hat{y}, e(x)]$  and extract hidden states from final token positions across all layers. We train diff-mean linear probes on these states, yielding layer-wise faithfulness representations  $\vec{F}_\ell$ . For classification tasks, we use class-averaged faithfulness vectors to isolate faithfulness-specific representations independent of class confounders. Based on these faithfulness vectors, we compute a majority vote across layer-wise linear probes beyond layer 5. Figure 2 shows faithfulness can be reliably detected across all evaluated tasks and models, with F1 scores ranging from 61.1% to 74.5%. This consistency suggests that NeuroFaith captures a systematic aspect of model behavior that manifests similarly across different tasks. Details about class-averaged faithfulness vectors and layer-wise classification score are in Appendix D.3.

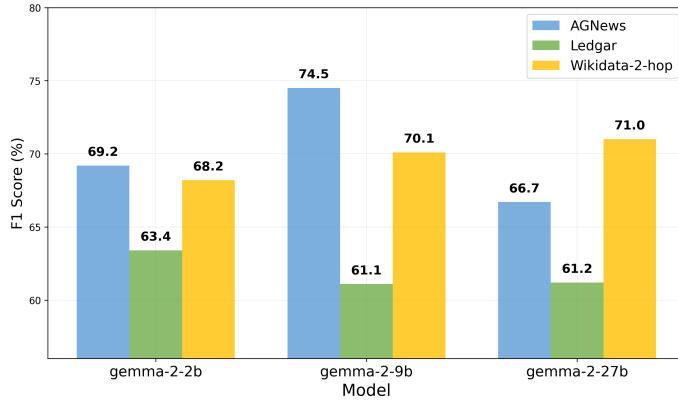


Figure 2: Majority vote faithfulness linear probe performance across models and datasets.

**Linear Representation Similarity Analysis.** To investigate the hypothesized relationships between faithfulness and related AI safety behaviors, we analyze the representational overlap between NeuroFaith faithfulness vectors and established linear representations of hallucination and deceptiveness from prior work (Rimsky et al., 2024; Goldowsky-Dill et al., 2025). Given that faithful explanations should accurately reflect model reasoning while hallucination and deceptiveness involve misrepresentation of information, we expect these behaviors to exhibit inverse correlations in their neural representations. We restrict analysis to layers with  $F1 > 60\%$  where faithfulness is properly linearly represented. Figure 3 shows maximum cosine similarity and corresponding layers for gemma-2-27B (additional results in Appendix D.3). Key findings emerge: Faithfulness vectors are consistently negatively correlated with hallucination and deceptiveness ones (up to  $-0.38$ ), aligning with expectations about the opposition between faithfulness and both deceptiveness and hallucination. Except Ledgar with 2-hop reasoning, cross-task faithfulness vectors show positive correlation ( $0.28$ - $0.49$ ), suggesting shared underlying representations of faithful reasoning across domains. These correlations validate that NeuroFaith captures behaviorally meaningful aspects of model reasoning aligned with established AI safety behaviors. Table 6 in Appendix D.3 corroborates these findings, demonstrating cross-task transfer: faithfulness vectors trained on 2-hop reasoning can detect unfaithful self-NLE in AGNews, and AGNews faithfulness vectors can detect unfaithful self-NLE in Ledgar (using gemma-2-27b).

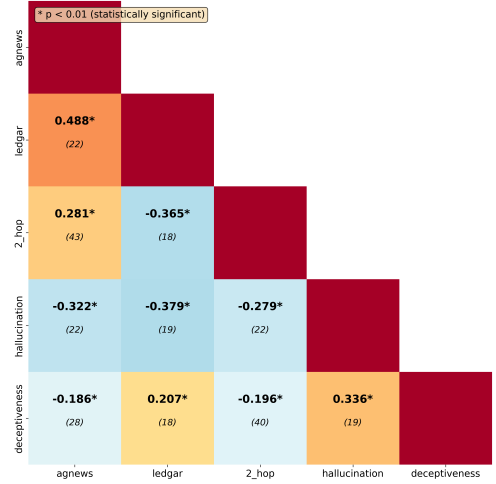


Figure 3: Linear vectors max. cosine similarity on gemma-2-27b

## 6.2 Faithfulness Enhancement Through Steering on 2-hop reasoning

Having established the linear structure of NeuroFaith faithfulness representations and their negative correlation with hallucination and deceptiveness vectors, we investigate whether linear steering can improve self-NLE faithfulness during inference. We implement activation steering by modifying hidden states during inference:  $h_k^\ell \leftarrow h_k^\ell + \lambda \times \overrightarrow{SV}_\ell$ , where  $\overrightarrow{SV}_\ell$  is the steering vector and  $\lambda$  controls intervention intensity. Our objective is here to demonstrate immediate practical value for improving self-NLE faithfulness during inference without model modification. More sophisticated steering methods (Hedström et al., 2025) would likely yield superior results. We evaluate three approaches: *faithfulness amplification* ( $\overrightarrow{SV}_\ell = \overrightarrow{F}_\ell$ ,  $\lambda = 1$ ) and *hallucination/deceptiveness inhibition* ( $\overrightarrow{SV}_\ell = \overrightarrow{H}_\ell$  or  $\overrightarrow{D}_\ell$ ,  $\lambda = -1$ ), where  $\overrightarrow{H}_\ell$  and  $\overrightarrow{D}_\ell$  are hallucination and deceptiveness linear vectors obtained from Rimsky et al. (2024) and Goldowsky-Dill et al. (2025). Faithfulness intervention targets only layers with  $F1 > 60\%$ , ensuring modifications occur where faithfulness is reliably encoded.

Table 3 shows steering interventions successfully convert 8-11% of unfaithful self-NLE into faithful explanations across all models. Direct faithfulness amplification consistently outperforms hallucination and deceptiveness inhibition, indicating these are distinct behavioral dimensions. Steering effectiveness remains consistent regardless of pre-

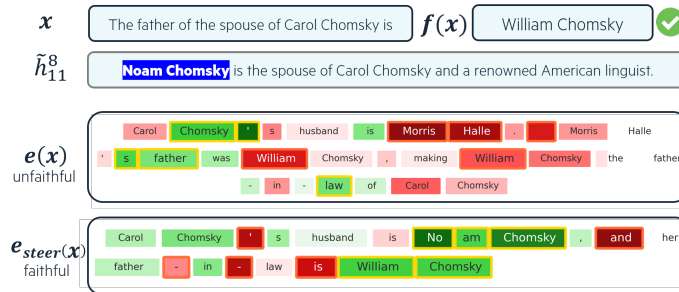


Figure 4: Faithfulness linear probe visualization examples before ( $e$ ) and after ( $e_{steer}$ ) faithfulness steering. Red: unfaithful activations; Green: faithful activations.

Model	Faithfulness $\lambda = 1$			Hallucination $\lambda = -1$			Deceptiveness $\lambda = -1$		
	acc.	inacc.	overall	acc.	inacc.	overall	acc.	inacc.	overall
gemma-2-2b	11.3%	9.3%	11.1%	10.0%	10.1%	10.0%	4.1%	5.7%	4.2%
gemma-2-9b	8.3%	10.8%	8.7%	8.0%	11.2%	8.5%	4.9%	2.5%	4.5%
gemma-2-27b	10.9%	11.3%	11.0%	9.2%	9.1%	9.2%	4.1%	3.2%	3.9%

Table 3: Proportion of initially unfaithful self-NLE made faithful through steering interventions.

diction accuracy, demonstrating genuine explanation quality improvements. Both methods show similar overall gains and highlight the practical utility of NeuroFaith for real-time faithfulness enhancement without model modification. Figure 4 shows how a faithfulness linear probe identifies bridge objects as key tokens determining self-NLE faithfulness, comparing an unfaithful example with its steered faithful version. Additional analyses include comprehensive faithfulness status changes and other examples of converted self-NLE (see Appendix E.1 and H).

## 7 Conclusion

This work introduces NeuroFaith, a flexible framework that measures self-NLE faithfulness by comparing explanations against mechanistic analysis of model internal activity. NeuroFaith aligns more closely than existing approaches with the common acceptance of faithfulness. Our key contributions suggest that faithfulness exhibits linear structure in LLM representation space, enabling both fast and reliable detection and enhancement through steering interventions. These findings establish concrete pathways toward more transparent AI systems, opening up new avenues of research on faithfulness. NeuroFaith relies on concept extraction methods that may introduce systematic biases, and circuit selection requires domain expertise or expensive circuit discovery that may limit generalizability. Our analysis focuses on *predict-then-explain* scenarios; extending to *explain-then-predict* settings could reveal how explanation faithfulness relates to performance gains (Bhan et al., 2024). Additionally, applying NeuroFaith to chain-of-thought reasoning could provide valuable comparisons with existing CoT faithfulness studies (Lanham et al., 2023; Turpin et al., 2023), advancing our understanding of reasoning faithfulness.

## References

- Chirag Agarwal, Sree Harsha Tanneru, and Himabindu Lakkaraju. Faithfulness vs. plausibility: On the (un) reliability of explanations from large language models. *arXiv preprint arXiv:2402.04614*, 2024.
- Pepa Atanasova, Oana-Maria Camburu, Christina Lioma, Thomas Lukasiewicz, Jakob Grue Simonsen, and Isabelle Augenstein. Faithfulness Tests for Natural Language Explanations. In Anna Rogers, Jordan Boyd-Graber, and Naoaki Okazaki (eds.), *Proc. of the 61st Annual Meeting of the Association for Computational Linguistics (Volume 2: Short Papers)*, pp. 283–294, Toronto, Canada, July 2023. Association for Computational Linguistics. doi: 10.18653/v1/2023.acl-short.25. URL <https://aclanthology.org/2023.acl-short.25>.
- Yonatan Belinkov. Probing classifiers: Promises, shortcomings, and advances. *Computational Linguistics*, 48(1): 207–219, 2022.
- Nora Belrose, David Schneider-Joseph, Shauli Ravfogel, Ryan Cotterell, Edward Raff, and Stella Biderman. Leace: Perfect linear concept erasure in closed form. *Advances in Neural Information Processing Systems*, 36:66044–66063, 2023.

- Leonard Bereska and Stratis Gavves. Mechanistic interpretability for ai safety-a review. *Transactions on Machine Learning Research*, 2024.
- Milan Bhan, Jean-Noël Vittaut, Nicolas Chesneau, and Marie-Jeanne Lesot. Self-AMPLIFY: Improving small language models with self post hoc explanations. In Yaser Al-Onaizan, Mohit Bansal, and Yun-Nung Chen (eds.), *Proceedings of the 2024 Conference on Empirical Methods in Natural Language Processing*, pp. 10974–10991, Miami, Florida, USA, November 2024. Association for Computational Linguistics. doi: 10.18653/v1/2024.emnlp-main.615. URL <https://aclanthology.org/2024.emnlp-main.615/>.
- Milan Bhan, Yann Choho, Pierre Moreau, Jean-Noel Vittaut, Nicolas Chesneau, and Marie-Jeanne Lesot. Towards achieving concept completeness for textual concept bottleneck models. In *Findings of the 2025 Conference on Empirical Methods in Natural Language Processing*. Association for Computational Linguistics, November 2025.
- Przemyslaw Biecek and Wojciech Samek. Position: explain to question not to justify. In *Proceedings of the 41st International Conference on Machine Learning*, pp. 3996–4006, 2024.
- Eden Biran, Daniela Gottesman, Sohee Yang, Mor Geva, and Amir Globerson. Hopping too late: Exploring the limitations of large language models on multi-hop queries. In *Proceedings of the 2024 Conference on Empirical Methods in Natural Language Processing*, pp. 14113–14130, 2024.
- Haozhe Chen, Carl Vondrick, and Chengzhi Mao. Selfie: Self-interpretation of large language model embeddings. In *Forty-first International Conference on Machine Learning*, 2024.
- Arthur Conmy, Augustine Mavor-Parker, Aengus Lynch, Stefan Heimersheim, and Adrià Garriga-Alonso. Towards automated circuit discovery for mechanistic interpretability. *Advances in Neural Information Processing Systems*, 36:16318–16352, 2023.
- Jacob Dunefsky, Philippe Chlenski, and Neel Nanda. Transcoders find interpretable llm feature circuits. In *The Thirty-eighth Annual Conference on Neural Information Processing Systems*, 2024.
- Nelson Elhage, Neel Nanda, Catherine Olsson, Tom Henighan, Nicholas Joseph, Ben Mann, Amanda Askell, Yuntao Bai, Anna Chen, Tom Conerly, Nova DasSarma, Dawn Drain, Deep Ganguli, Zac Hatfield-Dodds, Danny Hernandez, Andy Jones, Jackson Kernion, Liane Lovitt, Kamal Ndousse, Dario Amodei, Tom Brown, Jack Clark, Jared Kaplan, Sam McCandlish, and Chris Olah. A mathematical framework for transformer circuits. *Transformer Circuits Thread*, 2021. <https://transformer-circuits.pub/2021/framework/index.html>.
- Nelson Elhage, Tristan Hume, Catherine Olsson, Nicholas Schiefer, Tom Henighan, Shauna Kravec, Zac Hatfield-Dodds, Robert Lasenby, Dawn Drain, Carol Chen, Roger Grosse, Sam McCandlish, Jared Kaplan, Dario Amodei, Martin Wattenberg, and Christopher Olah. Toy models of superposition. *Transformer Circuits Thread*, 2022. [https://transformer-circuits.pub/2022/toy\\_model/index.html](https://transformer-circuits.pub/2022/toy_model/index.html).
- Javier Ferrando and Elena Voita. Information flow routes: Automatically interpreting language models at scale. In *Proceedings of the 2024 Conference on Empirical Methods in Natural Language Processing*, pp. 17432–17445, 2024.
- Atticus Geiger, Duligur Ibeling, Amir Zur, Maheep Chaudhary, Sonakshi Chauhan, Jing Huang, Aryaman Arora, Zhengxuan Wu, Noah Goodman, Christopher Potts, et al. Causal abstraction: A theoretical foundation for mechanistic interpretability. *Journal of Machine Learning Research*, 26(83):1–64, 2025.
- Robert Geirhos, Jörn-Henrik Jacobsen, Claudio Michaelis, Richard Zemel, Wieland Brendel, Matthias Bethge, and Felix A Wichmann. Shortcut learning in deep neural networks. *Nature Machine Intelligence*, 2(11):665–673, 2020.
- Asma Ghandeharioun, Avi Caciularu, Adam Pearce, Lucas Dixon, and Mor Geva. Patchscopes: A unifying framework for inspecting hidden representations of language models. In *Forty-first International Conference on Machine Learning*, 2024.
- Joseph Goguen. What is a concept? In *Proceedings of the 13th international conference on Conceptual Structures: common Semantics for Sharing Knowledge*, pp. 52–77, 2005.
- Nicholas Goldowsky-Dill, Bilal Chughtai, Stefan Heimersheim, and Marius Hobbhahn. Detecting strategic deception with linear probes. In *Forty-second International Conference on Machine Learning*, 2025.
- M. Grabisch, J.-L. Marichal, R. Mesiar, and E. Pap. *Aggregation functions*, volume 127. Cambridge University Press, 2009.
- Jiawei Gu, Xuhui Jiang, Zhichao Shi, Hexiang Tan, Xuehao Zhai, Chengjin Xu, Wei Li, Yinghan Shen, Shengjie Ma, Honghao Liu, et al. A survey on llm-as-a-judge. *arXiv preprint arXiv:2411.15594*, 2024.
- Antonio Gulli. Ag’s corpus of news articles. *Dipartimento di Informatica, University of Pisa, Nov*, 2005.

- Tessa Han, Yasha Ektefaie, Maha Farhat, Marinka Zitnik, and Himabindu Lakkaraju. Is ignorance bliss? the role of post hoc explanation faithfulness and alignment in model trust in laypeople and domain experts. *arXiv preprint arXiv:2312.05690*, 2023.
- Anna Hedström, Salim I Amoukou, Tom Bewley, Saumitra Mishra, and Manuela Veloso. To steer or not to steer? mechanistic error reduction with abstention for language models. In *Forty-second International Conference on Machine Learning*, 2025.
- Shiyuan Huang, Siddarth Mamidanna, Shreedhar Jangam, Yilun Zhou, and Leilani H. Gilpin. Can Large Language Models Explain Themselves? A Study of LLM-Generated Self-Explanations, October 2023. URL <http://arxiv.org/abs/2310.11207>. arXiv:2310.11207 [cs].
- Alon Jacovi and Yoav Goldberg. Towards faithfully interpretable nlp systems: How should we define and evaluate faithfulness? In *Proceedings of the 58th Annual Meeting of the Association for Computational Linguistics*. Association for Computational Linguistics, 2020.
- Maxime Kayser, Bayar Menzat, Cornelius Emde, Bogdan Bercean, Alex Novak, Abdalá Morgado, Bartłomiej Papież, Susanne Gaube, Thomas Lukasiewicz, and Oana-Maria Camburu. Fool me once? contrasting textual and visual explanations in a clinical decision-support setting. In *Proceedings of the 2024 Conference on Empirical Methods in Natural Language Processing*, pp. 18891–18919, 2024.
- Been Kim, Martin Wattenberg, Justin Gilmer, Carrie Cai, James Wexler, Fernanda Viegas, et al. Interpretability beyond feature attribution: Quantitative testing with concept activation vectors (tcav). In *International conference on machine learning*, pp. 2668–2677. PMLR, 2018.
- Tamera Lanham, Anna Chen, Ansh Radhakrishnan, Benoit Steiner, Carson Denison, Danny Hernandez, Dustin Li, Esin Durmus, Evan Hubinger, Jackson Kernion, et al. Measuring faithfulness in chain-of-thought reasoning. *arXiv preprint arXiv:2307.13702*, 2023.
- Sijia Liu, Yuanshun Yao, Jinghan Jia, Stephen Casper, Nathalie Baracaldo, Peter Hase, Yuguang Yao, Chris Yuhao Liu, Xiaojun Xu, Hang Li, et al. Rethinking machine unlearning for large language models. *Nature Machine Intelligence*, pp. 1–14, 2025.
- Scott M. Lundberg and Su-In Lee. A unified approach to interpreting model predictions. In *Proc. of the 31st Int. Conf. on Neural Information Processing Systems*, NIPS’17, pp. 4768–4777, December 2017. ISBN 978-1-5108-6096-4. URL [https://papers.nips.cc/paper\\_files/paper/2017/file/8a20a8621978632d76c43dfd28b67767-Paper.pdf](https://papers.nips.cc/paper_files/paper/2017/file/8a20a8621978632d76c43dfd28b67767-Paper.pdf).
- Chu Fei Luo, Rohan Bhamhorja, Samuel Dahan, and Xiaodan Zhu. Evaluating explanation correctness in legal decision making. In *Canadian AI*, 2022.
- Qing Lyu, Marianna Apidianaki, and Chris Callison-Burch. Towards faithful model explanation in nlp: A survey. *Computational Linguistics*, pp. 1–67, 2024.
- Andreas Madsen, Sarath Chandar, and Siva Reddy. Are self-explanations from large language models faithful. In *Findings of the Association for Computational Linguistics: ACL 2024*, 2024.
- Katie Matton, Robert Ness, and Emre Kiciman. Walk the talk? measuring the faithfulness of large language model explanations. In *The Fourteenth International Conference on Learning Representations*, 2025.
- Vaibhav Mavi, Anubhav Jangra, and Adam Jatowt. Multi-hop question answering. *Foundations and Trends® in Information Retrieval*, 17(5):457–586, 2024.
- Kevin Meng, David Bau, Alex Andonian, and Yonatan Belinkov. Locating and editing factual associations in gpt. *Advances in neural information processing systems*, 35:17359–17372, 2022.
- Letitia Parcalabescu and Anette Frank. On measuring faithfulness or self-consistency of natural language explanations. In *Proceedings of the 62nd Annual Meeting of the Association for Computational Linguistics (Volume 1: Long Papers)*, pp. 6048–6089, 2024.
- Kiho Park, Yo Joong Choe, and Victor Veitch. The linear representation hypothesis and the geometry of large language models. In *Forty-first International Conference on Machine Learning*, 2024.
- Adam Paszke, Sam Gross, Francisco Massa, Adam Lerer, James Bradbury, Gregory Chanan, Trevor Killeen, Zeming Lin, Natalia Gimelshein, Luca Antiga, et al. Pytorch: An imperative style, high-performance deep learning library. *Advances in neural information processing systems*, 2019. URL <https://dl.acm.org/doi/10.5555/3454287.3455008>.
- Judea Pearl. *Causality*. Cambridge university press, 2009.

- Fabian Pedregosa, Gaël Varoquaux, Alexandre Gramfort, Vincent Michel, Bertrand Thirion, Olivier Grisel, Mathieu Blondel, Peter Prettenhofer, Ron Weiss, Vincent Dubourg, et al. Scikit-learn: Machine learning in python. *Journal of Machine Learning Research*, 12:2825–2830, 2011. URL <https://www.jmlr.org/papers/v12/pedregosa11a.html>.
- Alec Radford, Karthik Narasimhan, Tim Salimans, Ilya Sutskever, et al. Improving language understanding by generative pre-training. 2018.
- Daking Rai, Yilun Zhou, Shi Feng, Abulhair Saparov, and Ziyu Yao. A practical review of mechanistic interpretability for transformer-based language models. *arXiv preprint arXiv:2407.02646*, 2024.
- Tilman Räuher, Anson Ho, Stephen Casper, and Dylan Hadfield-Menell. Toward transparent ai: A survey on interpreting the inner structures of deep neural networks. In *2023 IEEE Conference on Secure and Trustworthy Machine Learning (SATML)*, pp. 464–483. IEEE, 2023.
- Marco Tulio Ribeiro, Sameer Singh, and Carlos Guestrin. ”Why Should I Trust You?”: Explaining the Predictions of Any Classifier. In *Proc. of the 22nd ACM SIGKDD Int. Conf. on Knowledge Discovery and Data Mining, KDD ’16*, pp. 1135–1144. Association for Computing Machinery, August 2016. ISBN 978-1-4503-4232-2. doi: 10.1145/2939672.2939778. URL <https://doi.org/10.1145/2939672.2939778>.
- Nina Rimsky, Nick Gabrieli, Julian Schulz, Meg Tong, Evan Hubinger, and Alexander Turner. Steering llama 2 via contrastive activation addition. In Lun-Wei Ku, Andre Martins, and Vivek Srikumar (eds.), *Proceedings of the 62nd Annual Meeting of the Association for Computational Linguistics (Volume 1: Long Papers)*, pp. 15504–15522, Bangkok, Thailand, August 2024. Association for Computational Linguistics. doi: 10.18653/v1/2024.acl-long.828. URL <https://aclanthology.org/2024.acl-long.828/>.
- Morgane Riviere, Shreya Pathak, Pier Giuseppe Sessa, Cassidy Hardin, Surya Bhupatiraju, Léonard Hussenot, Thomas Mesnard, Bobak Shahriari, Alexandre Ramé, et al. Gemma 2: Improving open language models at a practical size. *arXiv preprint arXiv:2408.00118*, 2024.
- Max Ruiz Luyten and Mihaela van der Schaar. A theoretical design of concept sets: improving the predictability of concept bottleneck models. *Advances in Neural Information Processing Systems*, 37:100160–100195, 2024.
- Pranab Sahoo, Prabhath Meharia, Akash Ghosh, Sriparna Saha, Vinija Jain, and Aman Chadha. A comprehensive survey of hallucination in large language, image, video and audio foundation models. In *Findings of the Association for Computational Linguistics: EMNLP 2024*, pp. 11709–11724, 2024.
- Noah Siegel, Oana-Maria Camburu, Nicolas Heess, and Maria Perez-Ortiz. The probabilities also matter: A more faithful metric for faithfulness of free-text explanations in large language models. In Lun-Wei Ku, Andre Martins, and Vivek Srikumar (eds.), *Proceedings of the 62nd Annual Meeting of the Association for Computational Linguistics (Volume 2: Short Papers)*, pp. 530–546, Bangkok, Thailand, August 2024. Association for Computational Linguistics. doi: 10.18653/v1/2024.acl-short.49. URL <https://aclanthology.org/2024.acl-short.49/>.
- Noah Y Siegel, Nicolas Heess, Maria Perez-Ortiz, and Oana-Maria Camburu. Faithfulness of llm self-explanations for commonsense tasks: Larger is better, and instruction-tuning allows trade-offs but not pareto dominance. *arXiv preprint arXiv:2503.13445*, 2025.
- Mukund Sundararajan, Ankur Taly, and Qiqi Yan. Axiomatic attribution for deep networks. In *Proc. of the 34th Int. Conf. on Machine Learning, ICML*, volume 70 of *ICML’17*, pp. 3319–3328. JMLR.org, August 2017. URL <https://proceedings.mlr.press/v70/sundararajan17a/sundararajan17a.pdf>.
- Harsh Trivedi, Niranjan Balasubramanian, Tushar Khot, and Ashish Sabharwal. MuSiQue: Multihop questions via single-hop question composition. *Transactions of the Association for Computational Linguistics*, 10:539–554, 2022. doi: 10.1162/tacl.a.00475. URL <https://aclanthology.org/2022.tacl-1.31/>.
- Don Tuggener, Pius Von Däniken, Thomas Peetz, and Mark Cieliebak. Ledger: a large-scale multi-label corpus for text classification of legal provisions in contracts. In *Proceedings of the twelfth language resources and evaluation conference*, pp. 1235–1241, 2020.
- Miles Turpin, Julian Michael, Ethan Perez, and Samuel Bowman. Language models don’t always say what they think: Unfaithful explanations in chain-of-thought prompting. *Advances in Neural Information Processing Systems*, 36: 74952–74965, 2023.
- Martin Tutek, Fateme Hashemi Chaleshtori, Ana Marasović, and Yonatan Belinkov. Measuring faithfulness of chains of thought by unlearning reasoning steps. *arXiv preprint arXiv:2502.14829*, 2025.
- Kevin Ro Wang, Alexandre Variengien, Arthur Conmy, Buck Shlegeris, and Jacob Steinhardt. Interpretability in the wild: a circuit for indirect object identification in gpt-2 small. In *The Eleventh International Conference on Learning Representations*, 2023.

- Sarah Wiegrefe and Ana Marasovic. Teach me to explain: A review of datasets for explainable natural language processing. In *Thirty-fifth Conference on Neural Information Processing Systems Datasets and Benchmarks Track (Round 1)*.
- Sarah Wiegrefe, Ana Marasović, and Noah A Smith. Measuring association between labels and free-text rationales. In *Proceedings of the 2021 Conference on Empirical Methods in Natural Language Processing*, pp. 10266–10284, 2021.
- Thomas Wolf, Lysandre Debut, Victor Sanh, Julien Chaumond, Clement Delangue, Anthony Moi, Pierric Cistac, Tim Rault, Rémi Louf, Morgan Funtowicz, et al. Transformers: State-of-the-art natural language processing. In *Proc. of the Conf. on Empirical Methods in Natural language Processing: system demonstrations, EMNLP*, pp. 38–45, 2020. URL <https://aclanthology.org/2020.emnlp-demos.6/>.
- Zhengxuan Wu, Aryaman Arora, Atticus Geiger, Zheng Wang, Jing Huang, Dan Jurafsky, Christopher D Manning, and Christopher Potts. Axbench: Steering llms? even simple baselines outperform sparse autoencoders. In *Forty-second International Conference on Machine Learning*, 2025.
- Sohee Yang, Elena Gribovskaya, Nora Kassner, Mor Geva, and Sebastian Riedel. Do large language models latently perform multi-hop reasoning? In *Proceedings of the 62nd Annual Meeting of the Association for Computational Linguistics (Volume 1: Long Papers)*, pp. 10210–10229, 2024.
- Wei Jie Yeo, Ranjan Satapathy, and Erik Cambria. Towards faithful natural language explanations: A study using activation patching in large language models. *arXiv preprint arXiv:2410.14155*, 2024.
- Andy Zou, Long Phan, Sarah Chen, James Campbell, Phillip Guo, Richard Ren, Alexander Pan, Xuwang Yin, Mantas Mazeika, Ann-Kathrin Dombrowski, et al. Representation engineering: A top-down approach to ai transparency. *arXiv preprint arXiv:2310.01405*, 2023.

## A Appendix

### Appendix Table of Contents

A	Scientific Libraries . . . . .	13
B	LLM Implementation Details . . . . .	13
C	Datasets . . . . .	14
D	NeuroFaith Implementation Details . . . . .	14
	D.1 Concept Extraction . . . . .	14
	D.2 Mechanistic Interpretation . . . . .	16
	D.3 Linear Latent Faithfulness Detection. . . . .	23
E	Detailed Taxonomy of Self-NLE in Two-hop Reasoning . . . . .	27
	E.1 2-hop reasoning detailed results. . . . .	29
F	NeuroFaith Faithfulness Measure Comparison . . . . .	33
	F.1 2-hop Reasoning Faithfulness Qualitative Comparison. . . . .	33
	F.2 2-hop Reasoning Faithfulness Quantitative Comparison. . . . .	34
G	Classification Examples . . . . .	36
H	2-hop Reasoning Taxonomy Examples . . . . .	37

### A Scientific Libraries

We used several open-source libraries in this work: pytorch (Paszke et al., 2019), HuggingFace transformers (Wolf et al., 2020) and sklearn Pedregosa et al. (2011).

### B LLM Implementation Details

**Backbone and Special Tokens.** The library used to import the pretrained autoregressive language models is Hugging-Face. In particular, the backbones version of Gemma-2-2B, Gemma-2-9B and Gemma-2-27B are

gemma-2-2B-it, gemma-2-9B-it, gemma-2-27B-it respectively. The models were imported with the Bfloat16 computational format. The following special tokens used were used for instruction prompting:

- `user_token= '<start_of_turn>user'`
- `assistant_token= '<start_of_turn>model'`
- `stop_token= '<eos>'`

**Text Generation.** Text generation was performed using the native functions of the Hugging Face library: `generate`. The `generate` function was used with the following parameters:

- `do_sample = True`
- `num_beams = 2`
- `no_repeat_ngram_size = 2`
- `repetition_penalty = 1.2`
- `early_stopping = True`
- `temperature = 0.05`

**Self-NLE Generation.** The prompt used to get self-NLE was as follows:

- `<user>`
- *Question*
- `<Assistant>`
- *Answer*
- `<user>`
- *"Give me a simple explanation of your answer."*
- `<Assistant>`

## C Datasets

Here we provide detailed information about the analyzed datasets. For 2-hop reasoning, we run NeuroFaith on the Wikidata-2-hop dataset (Biran et al., 2024). We first compute task accuracy on the whole dataset, and then sample 1500 accurate and inaccurate prediction for the following of our study. To sample these 1500 instances, we filter 2-hop reasoning questions where relations are subjective (e.g. *"the most notable work of"*) or equivocal, potentially leading to numerous possible answers (e.g. *"the work that features"*). We also sample by setting a maximum number of occurrences for generated answers (15), to foster diversity in the input questions. This filter enables to avoid having to many questions where the answer is a country (e.g. USA). We end up with a dataset made of 3000 samples with 1500 accurate and 1500 inaccurate predictions.

For classification, we run NeuroFaith on AGNews (Gulli, 2005), a newspaper article classification and Ledger (Tuggener et al., 2020), a more challenging critical domain legal document classification dataset. We retrieve the enriched versions from Bhan et al. (2025) with labeled concepts for CAV computation. For AGNews, the classes to predict are 'world', 'sport', 'business' and 'science & technology'. For Ledger, the classes to predict are "Amendments", "Survival", "Terminations" and "Terms". Each dataset is made of 4000 samples.

## D NeuroFaith Implementation Details

### D.1 Concept Extraction

Here we provide the prompts used to give instructions to Qwen-3-32b to extract relevant concepts (NeuroFaith step 1). For 2-hop reasoning, concept extraction consists in retrieving the bridge object from the self-NLE. Since the input text as the following structures :  $x = (o_1, r_1, \blacktriangle, r_2, \bullet)$ , we directly prompt the model to resolve  $(o_1, r_1, \blacktriangle)$  by grounding its response on the self-NLE only. We structure our prompt following an in-context learning template with two examples differing from the dataset of interest:

- `<user>`

- preprompt + preprompt\_example\_1
- <Assistant>
- *Emmanuel Macron*
- <user>
- preprompt + preprompt\_example\_2
- <Assistant>
- *Ingmar Bergman*
- preprompt +  $(o_1, r_1, \blacktriangle)$
- <user>

with preprompt = "Answer briefly and only according to the provided text. If there is no clear answer, say **\*\*no bridge object\*\***", preprompt\_example\_1 = "Emmanuel Macron is the president of Italy, and the capital city of Italy is Rome. **\*\* the president of Italy is**" and preprompt\_example\_2 = "The movie Persona is a movie happening in the Faro island and has been directed by Ingmar Bergman, who is from Sweden. **\*\*:** 'The director of Persona is"

For classification, we assess having access to a set of relevant concepts  $\mathcal{C}$  and labels related to the task of interest. Given a certain concept  $c$ , we only prompt the model to assess if the concept is present in the self-NLE if the concept was initially present in the input text, making the concept extraction process computationally less expansive. We structure our prompt following an in-context learning template with three examples differing from the dataset of interest:

- <user>
- preprompt + preprompt\_example\_1
- <Assistant>
- *YES*
- <user>
- preprompt + preprompt\_example\_2
- <Assistant>
- *YES*
- <user>
- preprompt + preprompt\_example\_3
- <Assistant>
- *NO*
- <user>
- preprompt + context\_extraction\_prompt( $\hat{y}, e(x), c$ )

with preprompt = "Analyze whether a given concept has a meaningful impact on predicting a specific category from the provided text explanation. Instructions: (1) Answer with exactly "YES" if the concept is clearly mentioned in the given text and relevant to the category prediction, (2) Answer with exactly "NO" if the concept is neither mentioned nor relevant in the given text (3) Consider the logical connection between the concept and the category in the given text".

For AGNews:

- preprompt\_example\_1 = "Text explanation: 'The article says that OECD countries became richer in the 20th century. This falls under the category of world'. Question: According to the previous text, does the concept "economic trends" have a meaningful impact on predicting the "world" category?"
- preprompt\_example\_2 = "Text explanation: 'The abstract underlines that the French soccer striker is a good player. It is relevant to sport'. Question: According to the previous text, does the concept "jargon specific to the sport" have a meaningful impact on predicting the "sport" category?"
- preprompt\_example\_3 = "Text explanation: 'The research paper discusses quantum computing algorithms and their complexity. This falls under the category of technology'. Question: According to the previous text, does the concept "cooking techniques" have a meaningful impact on predicting the "technology" category?"

For Ledger:

- `preprompt_example_1` = "Text explanation: 'This clause defines what happens to your stock options if your employment ends \*before\* they are fully vested. It's part of the core **terms** of your employment agreement that outlines how these shares work.' Question: According to the previous text, does the legal concept "Minimum commitment periods" have a meaningful impact on predicting the "terms" category?"
- `preprompt_example_2` = "Text explanation: 'This clause defines what happens to your stock options if your employment ends \*before\* they are fully vested. It's part of the core **terms** of your employment agreement that outlines how these shares work.' Question: According to the previous text, does the legal concept "Effect of termination" have a meaningful impact on predicting the "terms" category?"
- `preprompt_example_3` = "Text explanation: 'The clause specifically talks about how changes can be made to the agreement: "terminated, amended, modified or supplemented". These are all words that mean changing the original terms of the contract. Since it focuses on how the contract itself can be altered, the relevant category is **Amendments**' Question: According to the previous text, does the legal concept "Amendment procedures" have a meaningful impact on predicting the "Amendments" category?"

Finally, given a prediction  $\hat{y}$ , and self NLE  $e(x)$  and a concept  $c$ , `context_extraction_prompt`( $\hat{y}, e(x), c$ ) = "Text explanation:  $e(x)$ . Question: According to the previous text, does the concept  $c$  have a meaningful impact on predicting the  $\hat{y}$  category?"

## D.2 Mechanistic Interpretation

Here we provide implementation details about mechanistic interpretations of extracted concepts (NeuroFaith step 2).

**Circuit Granularity.** To generate an mechanistic interpretation of an LLM hidden state, the first step is to define the specific neural architectural component and granularity  $\mathcal{G}$ . Given an index  $k$  and a layer  $\ell$ , a granularity  $\mathcal{G}$  refers to a specific point within the model's computational subgraph where neural activations can be analyzed and from which a local neural interpretation  $i_k^\ell(x)$  is going to be generated. Transformer-based generative LLM can be viewed as a stack of decoder computational blocks (Radford et al., 2018). The information flow through a single layer and from a layer to another can be described with the following equations:

$$\begin{aligned} h_k^\ell &= h_k^{\ell-1} + a_k^\ell + m_k^\ell \\ a_k^\ell &= \text{MHA}^\ell(h_1^{\ell-1}, h_2^{\ell-1}, \dots, h_k^{\ell-1}) \\ m_k^\ell &= \text{MLP}^\ell(a_k^\ell + h_k^{\ell-1}) \end{aligned} \quad (1)$$

where  $h_k^\ell$  denotes the residual stream at index  $k$  and layer  $\ell$ ,  $a_k^\ell$  the attention output of the multi-head attention operation  $\text{MHA}^\ell$  and  $m_k^\ell$  the output from the multi-layer perceptron  $\text{MLP}^\ell$ .

This characterization of the information flow through a Transformer block naturally highlights three possible granularities, each offering different perspectives on the model's information processing: the residual stream (RS) focusing on  $h_k^\ell$ , which serves as the main information pathway through the network; the multi-head attention (MHA) focusing on  $a_k^\ell$ , which captures token-to-token interactions; and the multi-layer perceptron (MLP) focusing on  $m_k^\ell$  and performing non-linear transformations of the information (Elhage et al., 2021; Rai et al., 2024). These computational blocks offer a relevant granularity to decode the internal activity of an LLM, since focusing on neurons alone can rarely be done due to their polysemanticity (Elhage et al., 2022). Thus, a hidden state granularity is defined such as  $\mathcal{G} \in \{\text{RS}, \text{MHA}, \text{MLP}\}$ .

**Interpreter.** For the 2-hop reasoning instantiation, the interpreter used to decode  $f$  hidden states  $\{h_k^\ell\}$  is Patchscopes Ghandeharioun et al. (2024). We use the prompt "What is the following? Answer briefly [X,X]" to generate the interpretation where X is a token placeholder to be replaced in the latent space by the hidden state to be interpreted. We replace the placeholder tokens at layers 3 and 4 to get two interpretations per hidden state to decode. The layers to be interpreted by Patchscopes vary depending on the assessed model. We set the index token  $k$  as the last one related to  $o_1$  and focus on the late early layers as in Biran et al. (2024). This way,  $\ell \in \{5, 6, 7, 8, 9, 10, 11\}$  for `gemma-2-2B`,  $\ell \in \{8, 9, 10, 11, 12, 13, 14\}$  for `gemma-2-9B` and  $\ell \in \{11, 12, 13, 14, 15, 16, 17\}$  for `gemma-2-27B`.

For the classification instantiation and given a concept  $c$ , concept importance  $I_\Gamma(c)$  is based on the linear representation of the concept called CAV and denoted  $\vec{c}$ . Concepts are selected based on the identifiability of each concept on  $f$  representation space based on  $I_\Gamma(c)$ . Below are examples of selected concepts from Ledger and AGNews for `gemma-2-27b` with F1 score > 60%:

<b>Concept</b>	<b>Layer</b>	<b>F1 Score (%)</b>
Players	36	0.758
Political developments	43	0.842
Scores	10	0.626
Financial markets	35	0.758
Companies	36	0.805
Industry-specific terminology and jargon	34	0.745
Global issues	45	0.812
Sports events	45	0.854
Industry analysis	38	0.610
Economic trends	36	0.798
Industries	36	0.776
International events	36	0.847
Global politics	36	0.809
International relations	36	0.776
Foreign affairs	43	0.795
News about wars, conflicts	43	0.694
Athletic competitions	45	0.855
Teams	45	0.679
Game summaries	34	0.780
Jargon specific to the sport	45	0.854
Charts, graphs, and financial data	38	0.658
Advancements in computing	41	0.607
Technological trends	43	0.769

Table 4: Ledger concept max. F1 scores (&gt; 60%) with related layer for gemma-2-27b.

Concept	Layer	F1 Score (%)
Modification rights	34	0.838
Amendment procedures	39	0.803
Notice requirements	20	0.743
Approval mechanisms	28	0.816
Integration with original agreement	23	0.729
Format requirements	26	0.768
Severability of amendments	37	0.812
Retroactive application	27	0.638
Waiver limitations	30	0.793
Amendment thresholds	42	0.753
Amendment restrictions	36	0.730
Prior versions validity	45	0.759
Amendment documentation	24	0.759
Version control mechanisms	37	0.738
Material change provisions	33	0.754
Post-termination obligations	28	0.798
Duration of surviving terms	28	0.885
Identification of specific clauses	11	0.785
Indemnification continuation	40	0.862
Payment obligations survival	21	0.776
Non-compete/non-solicitation persistence	30	0.631
Representations/warranties survival	21	0.767
Remedies availability post-termination	42	0.845
Perpetual rights	40	0.815
Legal compliance requirements	34	0.721
Duration specifications	42	0.885
Commencement date	36	0.638
Expiration conditions	37	0.910
Renewal mechanisms	44	0.654
Term length	26	0.798
Condition precedents	28	0.798
Milestone-based periods	36	0.739
Initial term vs. renewal term distinctions	44	0.789
Evergreen provisions	13	0.768
Term modification triggers	28	0.728
Minimum commitment periods	34	0.777
Maximum term limitations	36	0.785
Regulatory term constraints	41	0.769
Term acceleration provisions	30	0.738
Rolling term provisions	29	0.823
Termination rights	28	0.888
Notice periods	45	0.726
Termination for convenience	44	0.677
Effect of termination	28	0.912
Wind-down procedures	28	0.865
Early termination penalties	36	0.682
Mutual termination provisions	27	0.854
Partial termination rights	37	0.833
Change of control provisions	29	0.729
Performance-based termination	44	0.719
Regulatory/legal change termination	15	0.776
Termination certification requirements	27	0.774
Post-termination restrictions	13	0.747
Transition obligations	28	0.856

Table 5: Ledger concept max. F1 scores (> 60%) with related layer for gamma-2-27b.

The concept importance  $I_{\Gamma}(c)$  can be either computed through representation engineering and concept erasure or gradient-based approaches such as TCAV. We perform concept erasure for  $\lambda \in [0,1]$  with a step size of 0.1. Table 4 and 5 show the F1 scores of the properly detected concepts in gemma-2-27b representation space. We estimate the attribution of  $c$  given circuit  $\Gamma$  as the  $\beta_1$  parameter of the following regression:  $p_{\hat{y}}(x, \{do(H_k^\ell = h_k^\ell - \lambda \times \vec{c}_\ell)\}_{(k,\ell) \in \Gamma}) = \beta_0 + \beta_1 \times \lambda$ . The t-test for  $\beta_1$  significance is expressed as follows:  $t = \frac{\hat{\beta}_1}{SE(\hat{\beta}_1)} = \frac{\hat{\beta}_1}{\sqrt{\frac{MSE}{\sum_{i=1}^n (\lambda_i - \bar{\lambda})^2}}}$ , where  $\lambda_i$  is the  $i$  realization of  $\lambda$  and  $\bar{\lambda}$  is the average  $\lambda$  on the analyzed sample. Figures 11 and 12 show the faithfulness distributions of NeuroFaith for AGNews and Ledger for gemma-2-27b.

The concept importance  $I_{\Gamma}(c)$  can also be computed with gradients-based approaches such as TCAV. It can be formally expressed based on the previously computed CAV  $\vec{c}$ .  $I_{\Gamma}(c)$  is calculated by aggregating the local importance measures related to the hidden states along circuit  $\Gamma$ :

$$I_{\Gamma}(c) = \bigodot_{(k,\ell) \in \Gamma} \langle \vec{c}, \nabla f_{\hat{y},k}^\ell(h_k^\ell) \rangle \quad (2)$$

where  $f_{\hat{y},k}^\ell$  is the sub-function from  $f$  taking  $h_k^\ell$  as input and generating the output  $p_{\hat{y}}$  and  $\bigodot$  an aggregation operator. The  $\bigodot$  operator represents the aggregation operator chosen according to the expected desired level of strictness to measure faithfulness. Among the many aggregation operators (see e.g. Grabisch et al. (2009)),  $\bigodot$  can be conjunctive (e.g. defined as the min function), disjunctive (e.g. the max function) or the average measure.

Faithfulness is finally calculated based on concept importance as follows:  $F(x, e) = \frac{1}{p} \sum_{i=1}^p \mathbf{1}_{I_{\Gamma}(c_i) > 0}$ . Below are two distributions of faithfulness for classification of self-NLE generated for AGnews and Ledger from gemma-2-27b.

In Figure 5, 6, 7, 8, 9, and 10 we plot the concepts sorted by frequency for faithful and unfaithful self-NLE for AGNews and Ledger for gemma-2-2b and gemma-2-9b for several class predictions. These figures enable to highlight concepts related to either faithful or unfaithful self-NLE. For example, Figure 8 highlights the concept of "companies" to the class world, which seems to be counterintuitive.

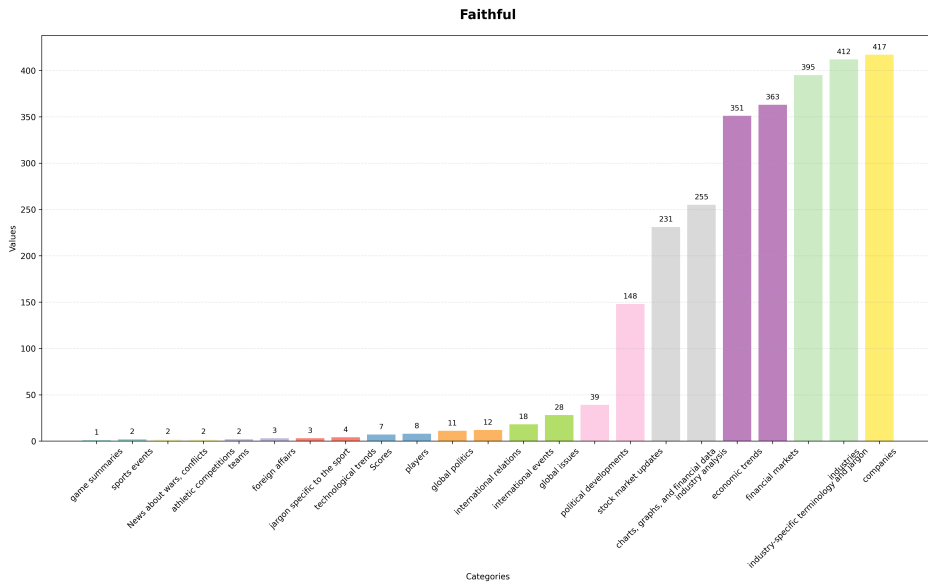


Figure 5: Concepts related to faithful self-NLE and the prediction "business", sorted by frequency for AGNews for gemma-2-2b.

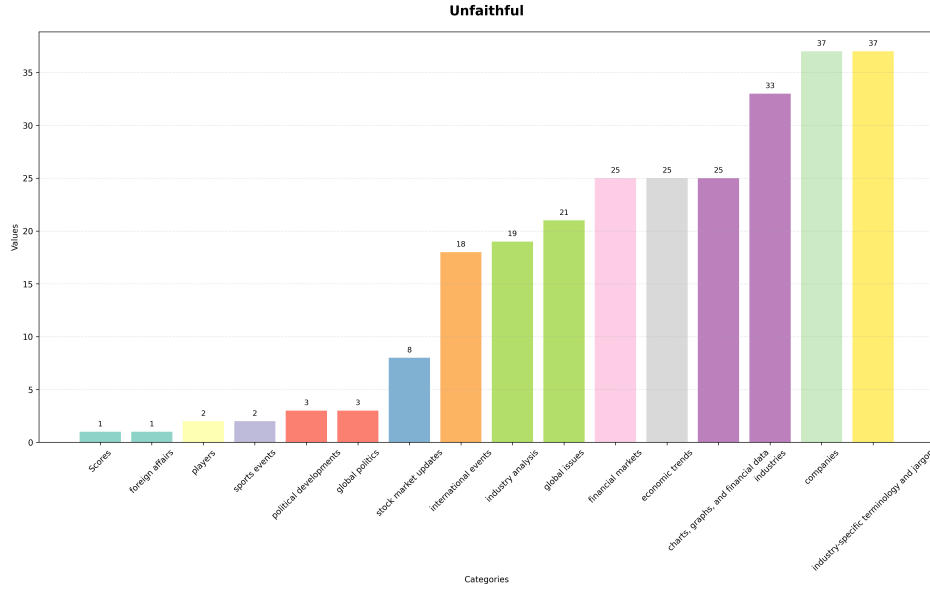


Figure 6: Concepts related to unfaithful self-NLE and the prediction "business", sorted by frequency for AGNews for gemma-2-2b.

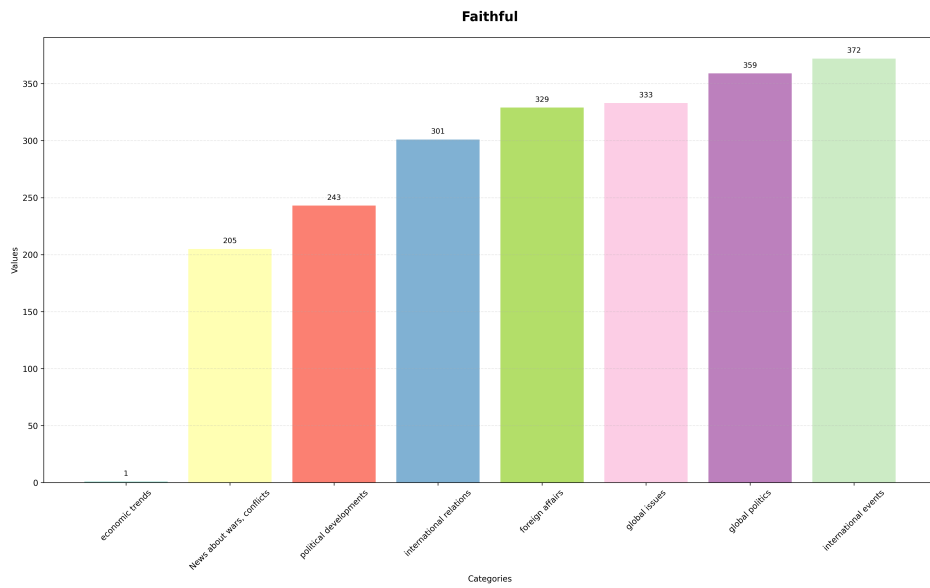


Figure 7: Concepts related to faithful self-NLE and the prediction "world", sorted by frequency for AGNews for gemma-2-2b.

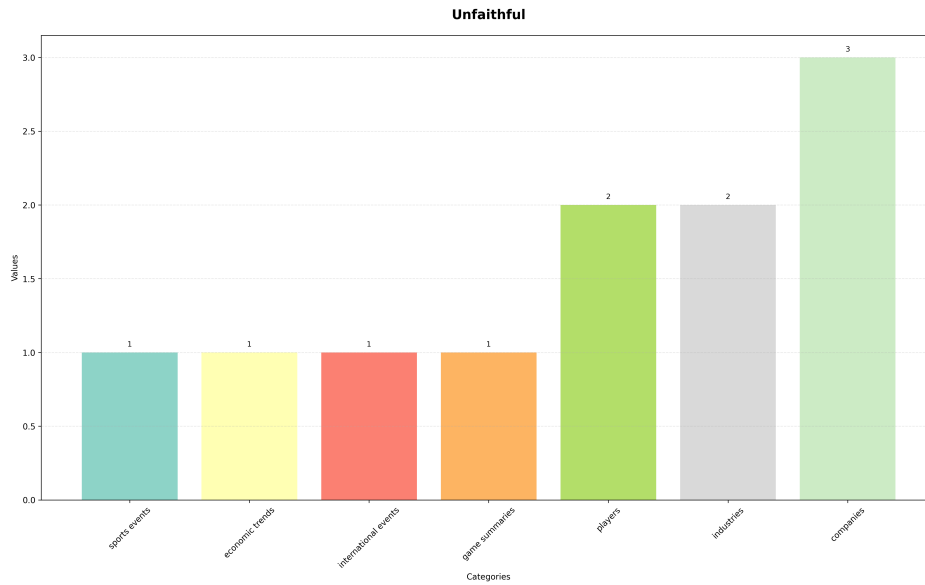


Figure 8: Concepts related to unfaithful self-NLE and the prediction "world", sorted by frequency for AGNews for gemma-2-2b.

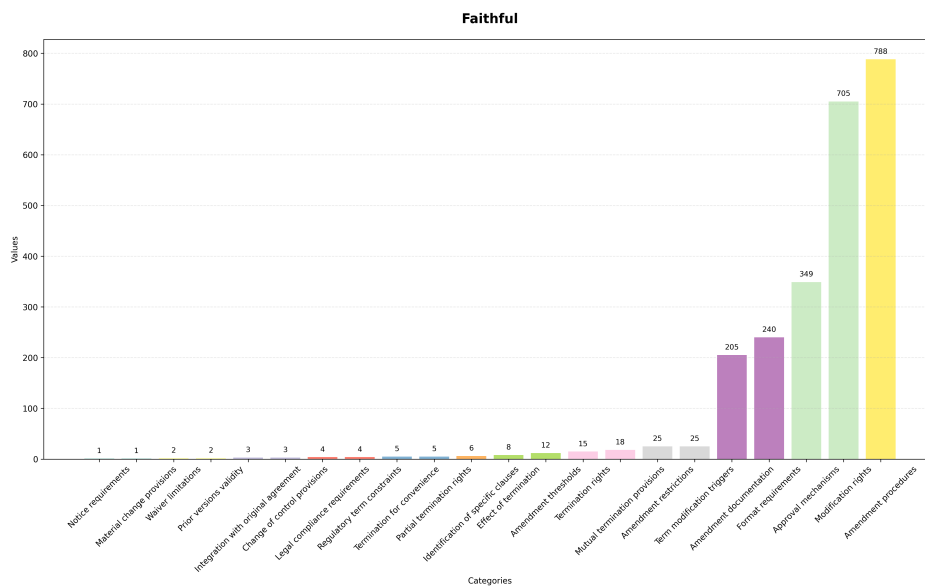


Figure 9: Concepts related to faithful self-NLE and the prediction "amendments", sorted by frequency for Ledger for gemma-2-9b.

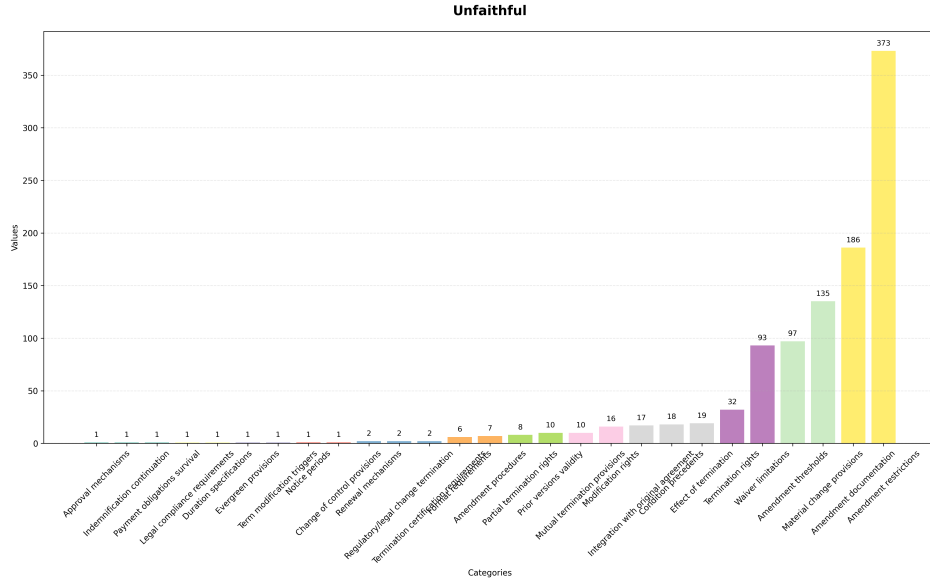


Figure 10: Concepts related to unfaithful self-NLE and the prediction "amendments", sorted by frequency for Ledger for gemma-2-9b.

We also plot the density of faithfulness for AGNews and Ledger for gemma-2-27b in Figure 11 and 12.

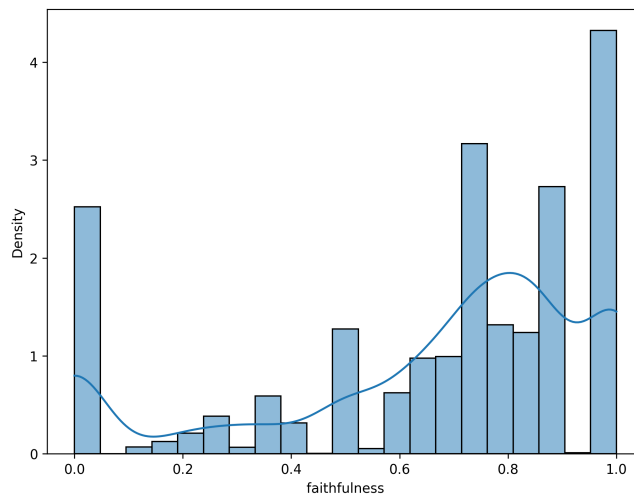


Figure 11: NeuroFaith faithfulness distribution for AGNews for gemma-2-27b.

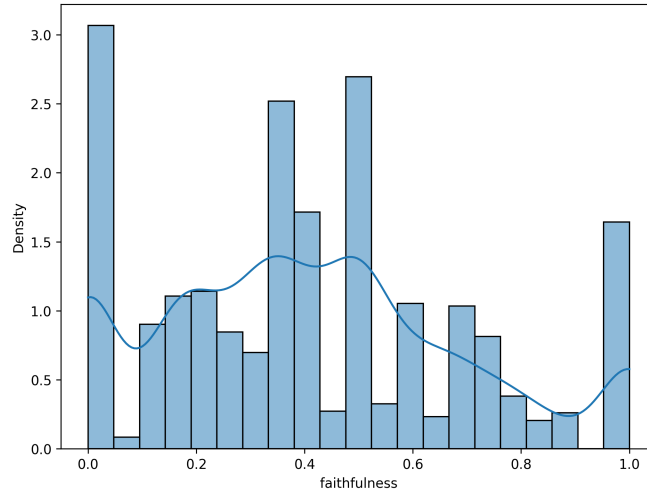


Figure 12: NeuroFaith faithfulness distribution for Ledger for gemma-2-27b.

### D.3 Linear Latent Faithfulness Detection.

Here we provide additional information about layer-wise linear probe performance and similarity between faithfulness vectors and with other AI safety linear vectors. Figures 13, 14, 15, 16, 17, 18, 19, 20, 21 show the layer-wise performance of the faithfulness linear probes for 2-hop reasoning, AGNews and Ledger. As shown in Figure 30, 23 and 31, cosine similarity between task-specific linear faithfulness and AI safety behaviors vectors becomes more pronounced with the size of the model.

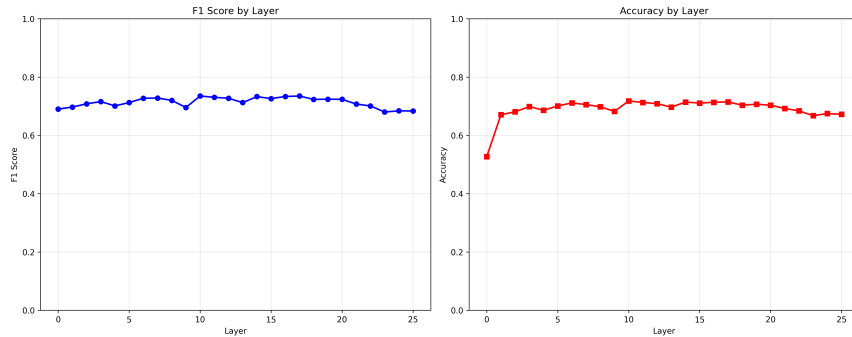


Figure 13: Linear faithfulness probe classification performance for 2-hop reasoning, gemma-2-2B.

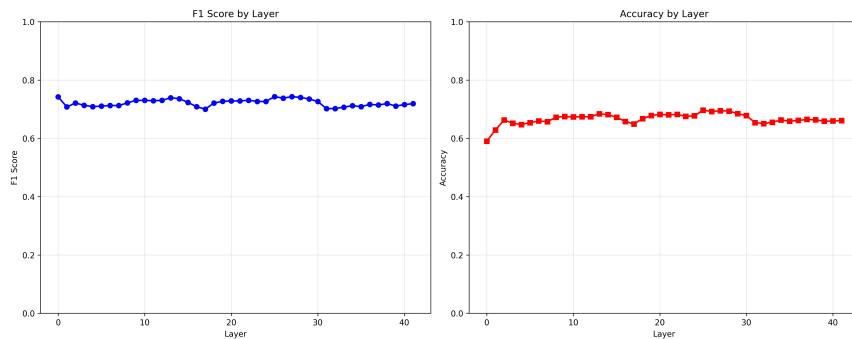


Figure 14: Linear faithfulness probe classification performance for 2-hop reasoning, gemma-2-9B.

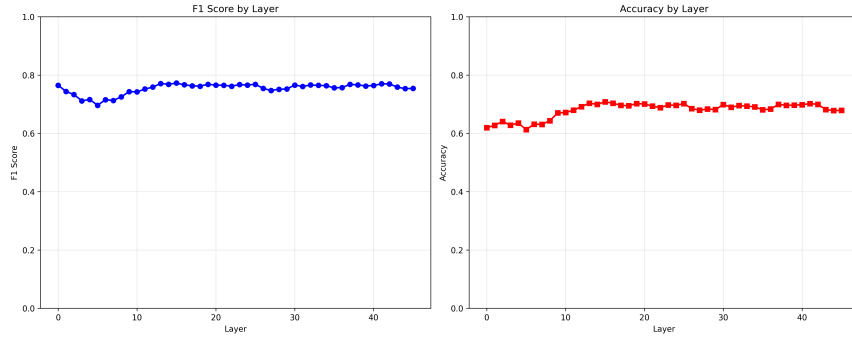


Figure 15: Linear faithfulness probe classification performance for 2-hop reasoning, gemma-2-27B.

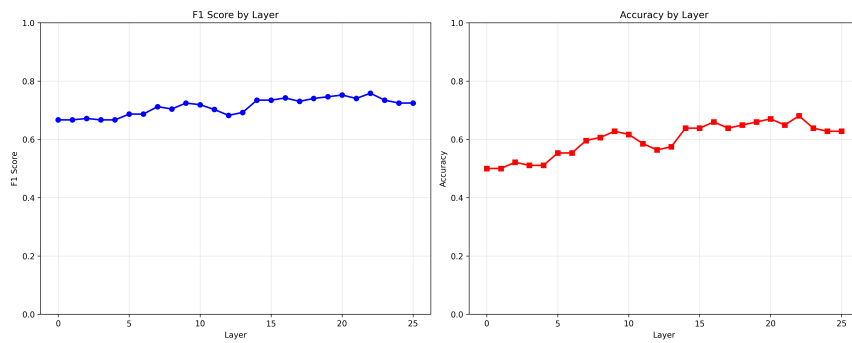


Figure 16: Linear faithfulness probe classification performance for AGNews classification, gemma-2-2B.

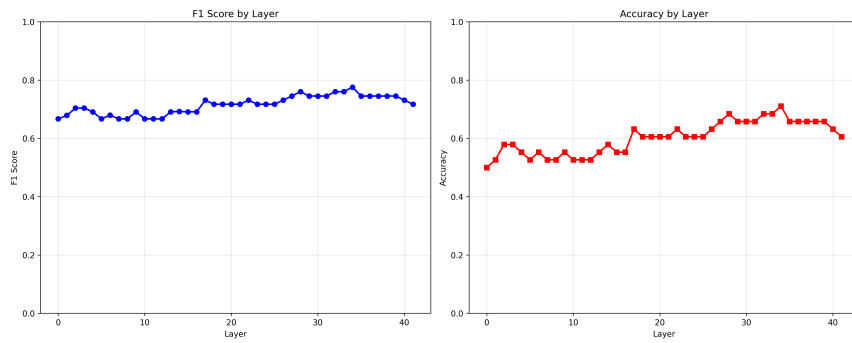


Figure 17: Linear faithfulness probe classification performance for AGNews classification, gemma-2-9B.

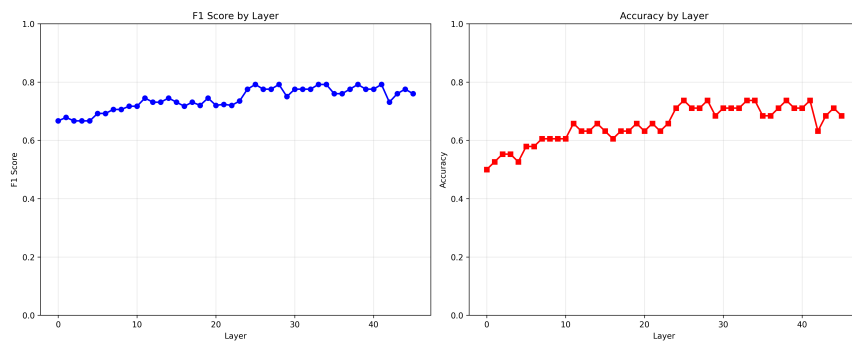


Figure 18: Linear faithfulness probe classification performance for AGNews classification, gemma-2-27B.

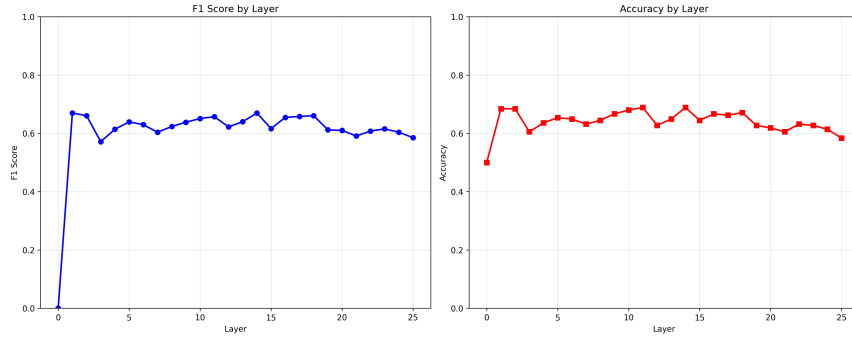


Figure 19: Linear faithfulness probe classification performance for Ledger classification, gemma-2-2B.

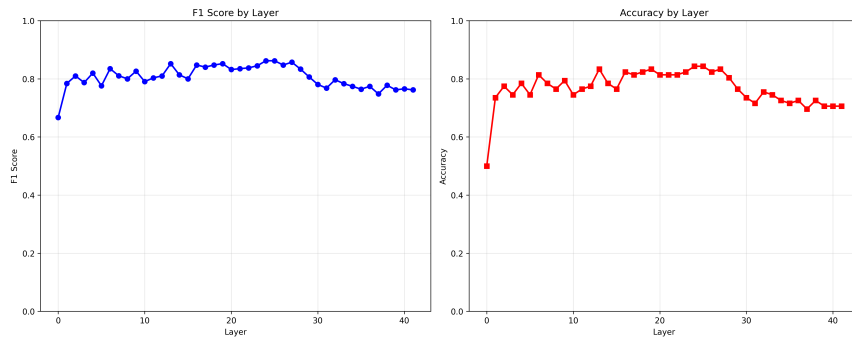


Figure 20: Linear faithfulness probe classification performance for Ledger classification, gemma-2-9B.

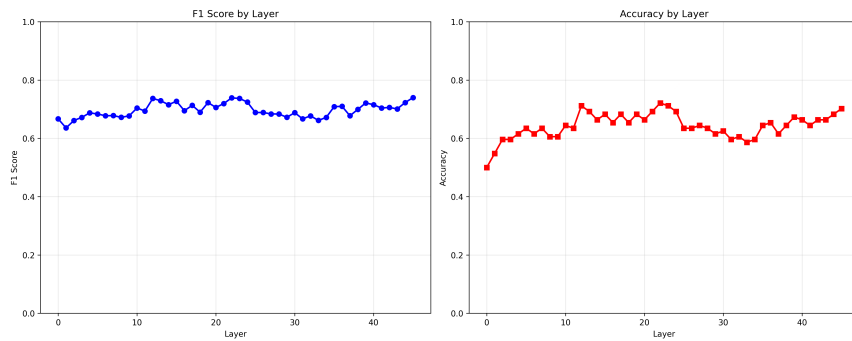


Figure 21: Linear faithfulness probe classification performance for Ledger classification, gemma-2-27B.

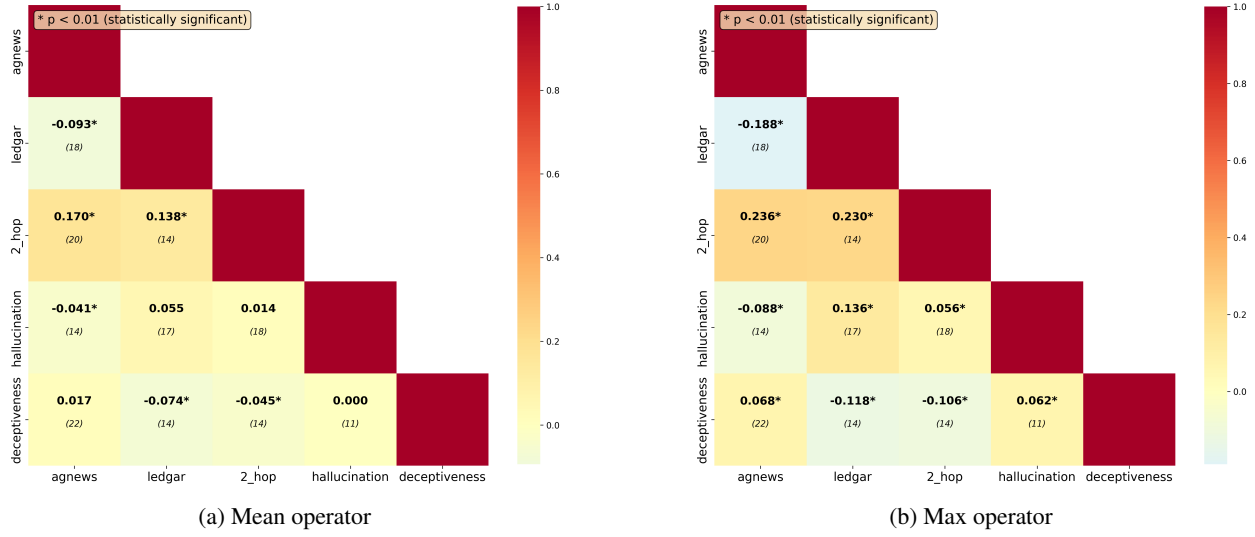


Figure 22: Linear vectors cosine similarity analysis on gemma-2-2b

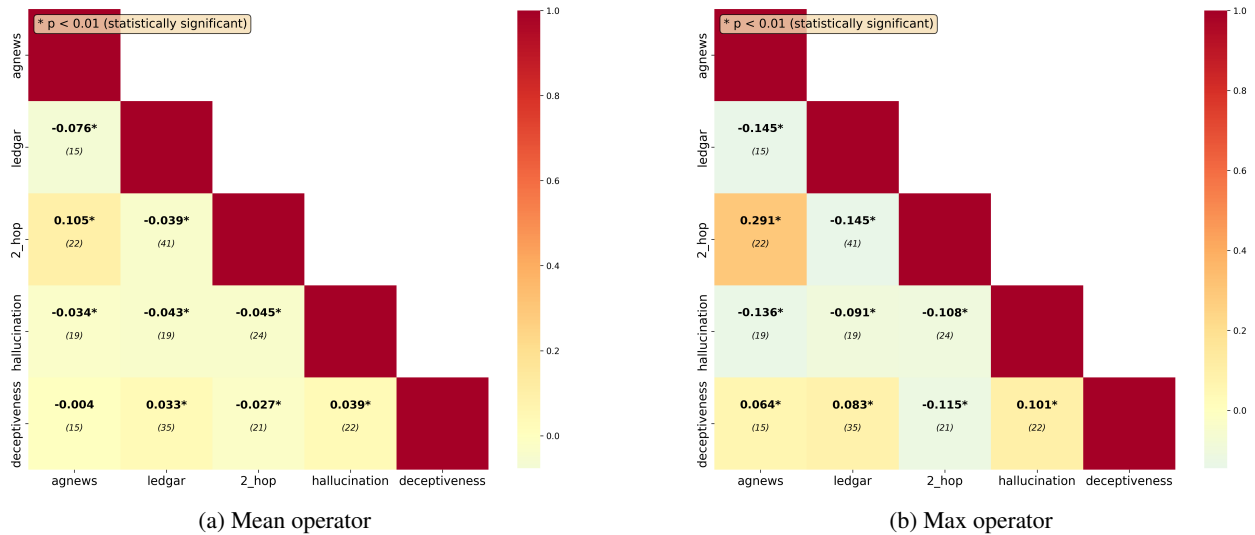


Figure 23: Linear vectors cosine similarity analysis on gemma-2-9b

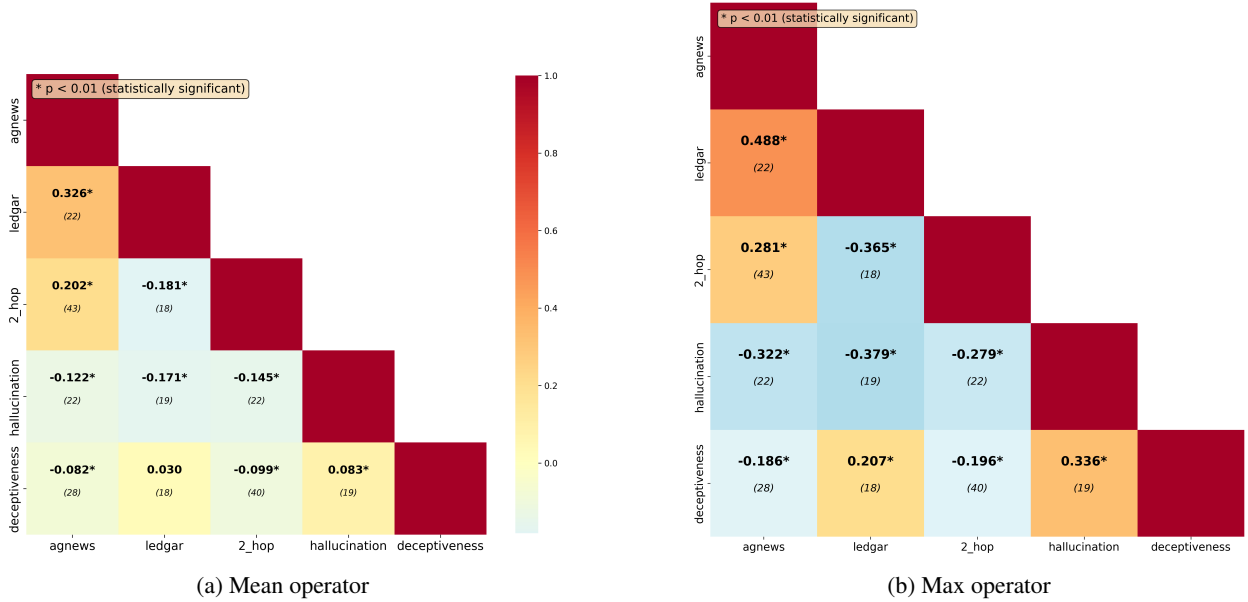


Figure 24: Linear vectors cosine similarity analysis on gemma-2-27b

Table 6 shows the F1 score for faithfulness linear detection by using the linear representation from one task (e.g. 2-hop reasoning) to predict self-NLE faithfulness from other tasks (e.g. Ledgar and AGNews). These results corroborate the cosine similarity analysis, highlighting that the 2-hop reasoning/AGNews and AGNews/Ledgar pairs are moderately correlated with gemma-2-27b, enabling to properly detect faithfulness (approximately 62%). This phenomenon does not appear on smaller models.

Base/Target	gemma-2b		gemma-9b		gemma-27b	
	Agnews	Ledgar	Agnews	Ledgar	Agnews	Ledgar
2-hop reasoning	52.2%	56.1%	47.2%	40.0%	61.3%	36.1%
AGNews	–	45.3%	–	42.2%	–	63.1%

Table 6: Faithfulness detection by transfer, from a base to a target faithfulness linear vector.

## E Detailed Taxonomy of Self-NLE in Two-hop Reasoning

**Taxonomy Definition.** The correctness of the prediction combined with both the faithfulness and the correctness of the self-NLE and the correctness of the first hop of the latent reasoning enables to precisely characterize  $e(x)$ . In this subsection, we focus on ten disjoint cases of interest to characterize the behavior of  $f$  with respect to  $e(x)$ . They are illustrated in Figure 25. Given a ground truth 2-hop reasoning trace  $(o_1, r_1, o_2, r_2, o_3)$  and the actual reasoning trace obtained from both the model answer and self-NLE:  $(o_1, r_1, \hat{o}_2, r_2, \hat{o}_3)$ :

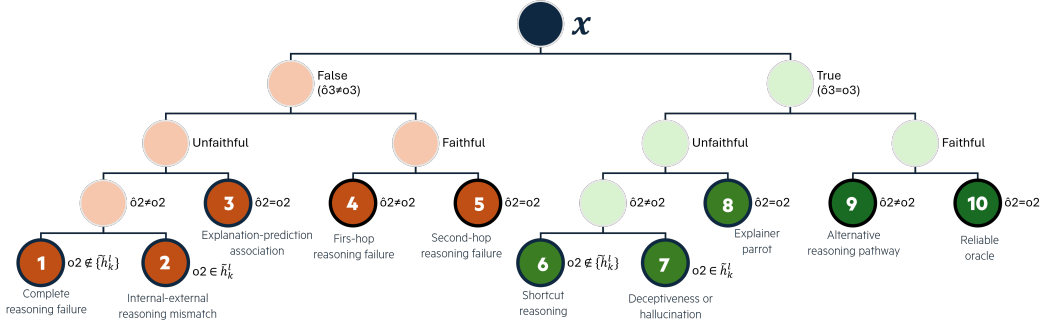


Figure 25: Detailed taxonomy of  $f$  behavior in two-hop reasoning, based on the status of the prediction, the self-NLE and the latent reasoning.

- **(C<sub>1</sub>) Complete reasoning failure.** If  $\hat{o}_3 \neq o_3$ ,  $F(x, e) = 0$ ,  $\hat{o}_2 \neq o_2$  and  $\forall(k, \ell) \in \Gamma, o_2 \notin \tilde{h}_k^\ell$ . *Observation:* Wrong prediction, incorrect unfaithful explanation, ground-truth bridge object undetected in circuit  $\Gamma$ . *Interpretation:* Evidence suggests failure in first-hop reasoning, with neither explanation nor internal representations containing the expected bridge object.
- **(C<sub>2</sub>) Internal-external reasoning mismatch.** If  $\hat{o}_3 \neq o_3$ ,  $F(x, e) = 0$ ,  $\hat{o}_2 \neq o_2$  and  $\exists(k, \ell) \in \Gamma, o_2 \in \tilde{h}_k^\ell$ . *Observation:* Wrong prediction, incorrect unfaithful explanation, but ground-truth bridge object detected in circuit  $\Gamma$ . *Interpretation:* Model appears to have correct internal knowledge but generates inconsistent explanations, indicating potential reasoning-explanation dissociation because of either deceptiveness or hallucination.
- **(C<sub>3</sub>) Explanation-prediction association.** If  $\hat{o}_3 \neq o_3$ ,  $F(x, e) = 0$  and  $\hat{o}_2 = o_2$ . *Observation:* Wrong prediction with unfaithful but correct explanation. *Interpretation:* Model associates correct bridge object with incorrect prediction during explanation generation, suggesting superficial pattern matching without genuinely resolving the first hop of the 2-hop reasoning.
- **(C<sub>4</sub>) First-hop reasoning failure.** If  $\hat{o}_3 \neq o_3$ ,  $F(x, e) = 1$  and  $\hat{o}_2 \neq o_2$ . *Observation:* Wrong prediction with faithful but incorrect explanation. *Interpretation:* Model consistently follows incorrect reasoning pathway, indicating systematic error in first-hop reasoning or concept misunderstanding.
- **(C<sub>5</sub>) Second-hop reasoning failure.** If  $\hat{o}_3 \neq o_3$ ,  $F(x, e) = 1$  and  $\hat{o}_2 = o_2$ . *Observation:* Wrong prediction with faithful and correct explanation. *Interpretation:* Model correctly identifies bridge object but fails in second reasoning step, suggesting error occurs after successful first-hop completion.
- **(C<sub>6</sub>) Shortcut learning.** If  $\hat{o}_3 = o_3$ ,  $F(x, e) = 0$ ,  $\hat{o}_2 \neq o_2$  and  $\forall(k, \ell) \in \Gamma, o_2 \notin \tilde{h}_k^\ell$ . *Observation:* Correct prediction with unfaithful incorrect explanation, ground-truth bridge object undetected. *Interpretation:* Evidence suggests direct  $o_1 \rightarrow o_3$  association, consistent with shortcut learning behavior that bypasses intermediate reasoning steps.
- **(C<sub>7</sub>) Deceptiveness or hallucination.** If  $\hat{o}_3 = o_3$ ,  $F(x, e) = 0$ ,  $\hat{o}_2 \neq o_2$  and  $\exists(k, \ell) \in \Gamma, o_2 \in \tilde{h}_k^\ell$ . *Observation:* Correct prediction with unfaithful incorrect explanation, but ground-truth bridge object detected internally. *Interpretation:* Model possesses correct internal knowledge but generates deceptive (or hallucinated) explanations, suggesting reasoning-explanation dissociation or alternative reasoning pathways. This case is expected to be rare, otherwise highlighting a case where  $f$  is not honest in its self-NLE while "knowing" the ground truth bridge object, raising a problem in  $f$  alignment.
- **(C<sub>8</sub>) Explainer parrot.** If  $\hat{o}_3 = o_3$ ,  $F(x, e) = 0$  and  $\hat{o}_2 = o_2$ . *Observation:* Correct prediction with unfaithful but correct explanation. *Interpretation:* Model generates expected explanations without corresponding detectable internal reasoning, suggesting post-hoc explanation generation (i.e. "explainer parrot" behavior).
- **(C<sub>9</sub>) Alternative reasoning pathway.** If  $\hat{o}_3 = o_3$ ,  $F(x, e) = 1$  and  $\hat{o}_2 \neq o_2$ . *Observation:* Correct prediction with faithful but incorrect explanation. *Interpretation:* Model uses consistent but non-canonical reasoning pathways, indicating systematic bias or alternative reasoning mechanism that leads to correct outcomes through unexpected intermediate steps.
- **(C<sub>10</sub>) Reliable oracle.** If  $\hat{o}_3 = o_3$ ,  $F(x, e) = 1$  and  $\hat{o}_2 = o_2$ . *Observation:* Correct prediction with faithful and correct explanation. *Interpretation:* Strong evidence for expected canonical reasoning pathway, representing the most interpretable and reliable case for knowledge extraction and model understanding.

Incorrect Predictions					
Model	C1 Complete reasoning failure	C2 Internal-external reasoning mismatch	C3 Explanation-prediction assoc.	C4 First-hop reasoning failure	C5 Second-hop reasoning failure
gemma-2-2b	23.8%	4.2%	14.4%	16.0%	41.6%
gemma-2-9b	26.1%	4.5%	14.5%	14.1%	40.9%
gemma-2-27b	22.8%	4.4%	12.5%	17.1%	43.1%

Table 7: Distribution of categories for incorrect predictions across model sizes.

Correct Predictions					
Model	C6 Shortcut learning	C7 Deceptiveness or hallucination	C8 Explainer parrot	C9 Alternative reasoning pathway	C10 Reliable oracle
gemma-2-2b	27.8%	6.1%	17.7%	8.1%	40.3%
gemma-2-9b	14.9%	4.2%	20.0%	6.8%	54.0%
gemma-2-27b	12.8%	3.1%	15.3%	6.4%	62.4%

Table 8: Distribution of categories for correct predictions across model sizes.

While this taxonomy relies on the interpreter ability to decode the model’s internal activity, the systematic patterns observed across different models and tasks provide convergent evidence for these behavioral categories. We give examples of this taxonomy in Appendix H

### E.1 2-hop reasoning detailed results.

Here we detail the results outlined in Section 4 and 6 by breaking down the results at the category-level as introduced above.

**Taxonomy Descriptive Analysis.** Table 7 highlights that the categories C1 (complete reasoning failure) and C5 (second-hop reasoning failure) are the most represented across the models. The distributions are overall highly stable for incorrect predictions whereas the category C10 (reliable oracle) increases with the model size for accurate predictions. The category C7 (deceptiveness or hallucination) tends to decrease with model size, but still represents a non negligible part of the self-NLE.

**Taxonomy Faithfulness Enhancement Analysis.** Table 9,10 and 11 respectively show the detailed impact of hallucination inhibition, linear faithfulness amplification and deceptiveness inhibition steering on self-NLE faithfulness. Categories C2 and C7 are the most prone to be turned into faithful self-NLE overall. Hallucination and faithfulness steering lead to significantly better results as compared to deceptiveness steering overall. Linear faithfulness amplification gives slightly better results than hallucination inhibition. Hallucination inhibition obtains slightly better results than linear faithfulness amplification for C1 and C6.

New Faithfulness After Steering Through Hallucination Inhibition (%)						
Model	C1 Complete reasoning failure	C2 Internal-external reasoning mismatch	C3 Explanation-prediction assoc.	C6 Shortcut learning	C7 Deceptiveness or hallucination	C8 Explainer parrot
gemma-2-2b	10.8%	<b>33.3%</b>	5.6%	7.4%	<b>36.2%</b>	3.0%
gemma-2-9b	9.2%	<b>13.4%</b>	5.1%	16.1%	<b>35.9%</b>	1.6%
gemma-2-27b	12.0%	<b>22.7%</b>	4.8%	12.5%	<b>48.9%</b>	2.6%

Table 9: Percentage of initially unfaithful explanations that become faithful after hallucination steering interventions, by category and model size.

New Faithfulness After Steering Through Linear Faithfulness Amplification (%)						
Model	C1 Complete reasoning failure	C2 Internal-external reasoning mismatch	C3 Explanation-prediction assoc.	C6 Shortcut learning	C7 Deceptiveness or hallucination	C8 Explainer parrot
gemma-2-2b	8.1%	<b>38.0%</b>	5.1%	9.3%	<b>39.5%</b>	1.1%
gemma-2-9b	6.9%	<b>28.4%</b>	3.7%	10.3%	<b>57.8%</b>	2.0%
gemma-2-27b	9.3%	<b>19.7%</b>	5.3%	10.9%	<b>40.4%</b>	1.3%

Table 10: Percentage of initially unfaithful explanations that become faithful after linear faithfulness steering interventions, by category and model size.

New Faithfulness After Steering Through Deceptiveness Inhibition (%)						
Model	C1 Complete reasoning failure	C2 Internal-external reasoning mismatch	C3 Explanation-prediction assoc.	C6 Shortcut learning	C7 Deceptiveness or hallucination	C8 Explainer parrot
gemma-2-2b	5.1%	3.2%	2.7%	4.7%	<b>13.8%</b>	6.0%
gemma-2-9b	6.1%	<b>11.7%</b>	0.6%	8.0%	<b>18.7%</b>	1.4%
gemma-2-27b	5.0%	6.3%	1.7%	2.7%	<b>9.1%</b>	3.3%

Table 11: Percentage of initially unfaithful explanations that become faithful after deceptiveness steering interventions, by category and model size (third experimental condition).

As shown in Figures 27, 28, and 29, we observe consistent transition patterns when steering makes unfaithful explanations faithful. For initially incorrect predictions, category C1 (complete reasoning failure) consistently transitions to C4 (first-hop reasoning failure), achieving faithfulness approximately 10% of the time under NeuroFaith linear faithfulness amplification and hallucination inhibition. Category C2 (internal-external reasoning mismatch) predominantly transitions to C5 (second-hop reasoning failure) when steering succeeds. Category C3 (explanation-prediction association) exclusively leads to C5 (second-hop reasoning failure) upon becoming faithful.

Initially accurate predictions follow similar patterns. Category C6 (shortcut learning) transitions to C9 (alternative reasoning pathway) when made faithful, while category C8 (explainer parrot) becomes C10 (reliable oracle). Category C7 (deceptiveness or hallucination) can transition to either C9 or C10, though it more commonly becomes a reliable oracle (C10). We give several examples of unfaithful self-NLE made faithful in Appendi H.

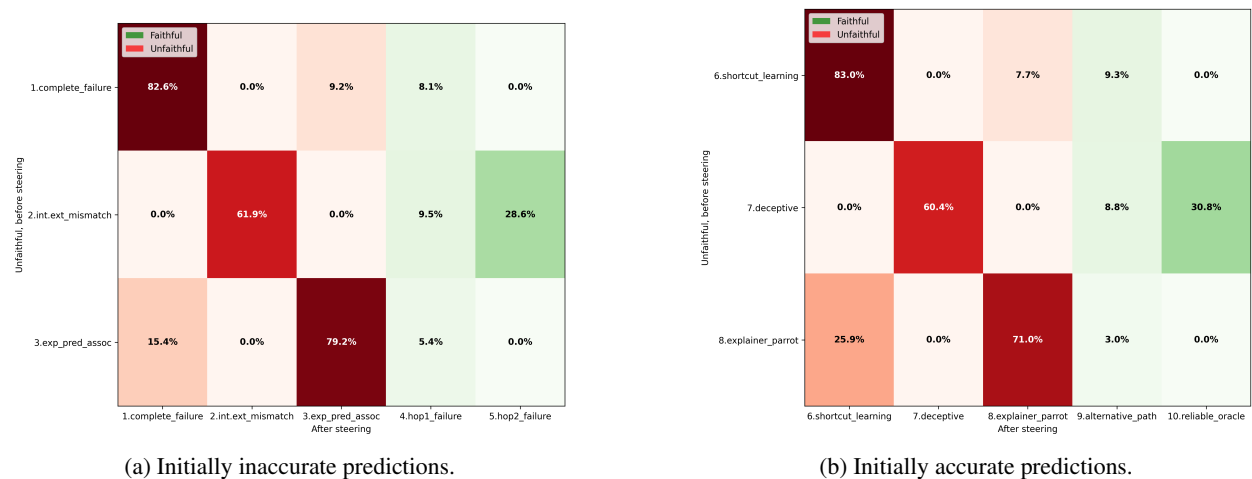
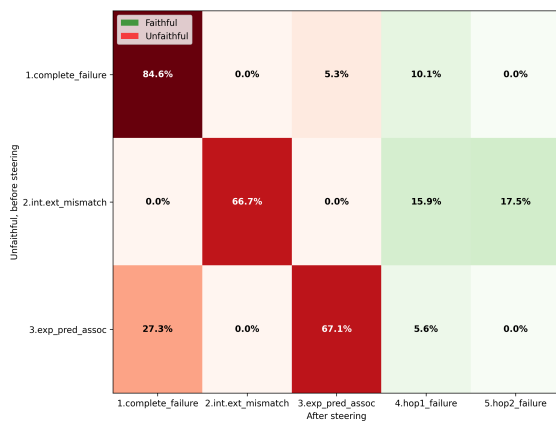
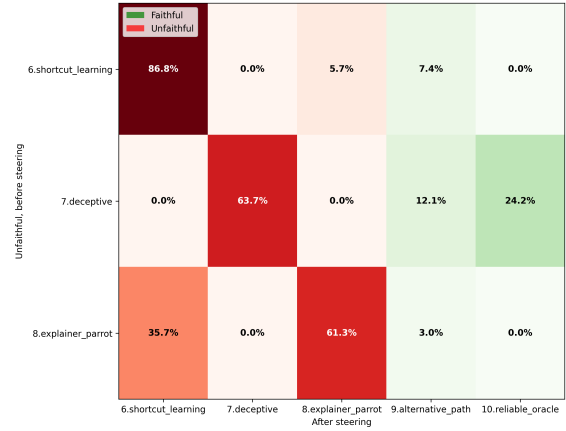


Figure 26: Detailed taxonomy transition state analysis, before and after NeuroFaith linear faithfulness steering on gemma-2-2b on 2-hop reasoning.

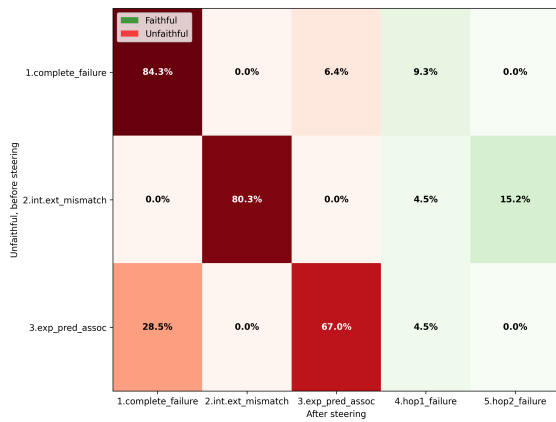


(a) Initially inaccurate predictions.

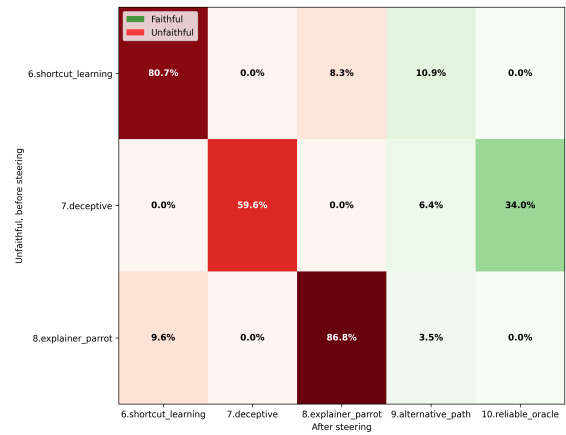


(b) Initially accurate predictions.

Figure 27: Detailed taxonomy transition state analysis, before and after hallucination inhibition on gemma-2-2b on 2-hop reasoning.

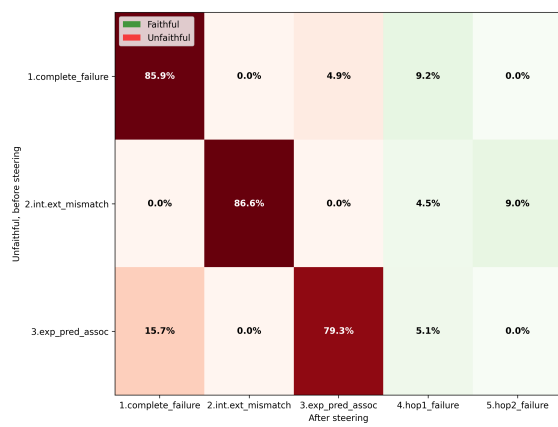


(a) Initially inaccurate predictions.

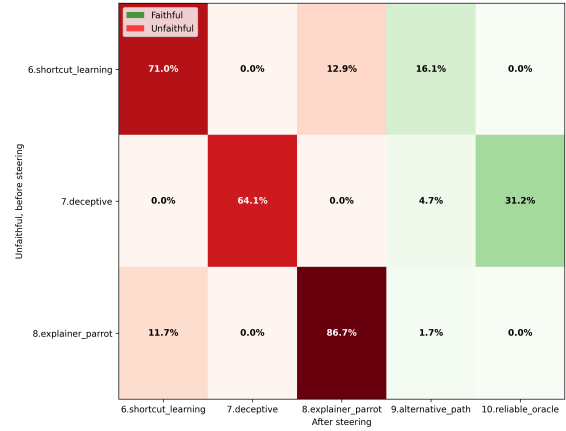


(b) Initially accurate predictions.

Figure 28: Detailed taxonomy transition state analysis, before and after NeuroFaith linear faithfulness steering on gemma-2-9b on 2-hop reasoning.

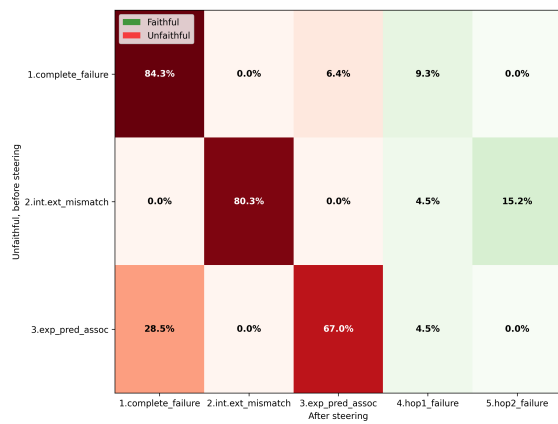


(a) Initially inaccurate predictions.

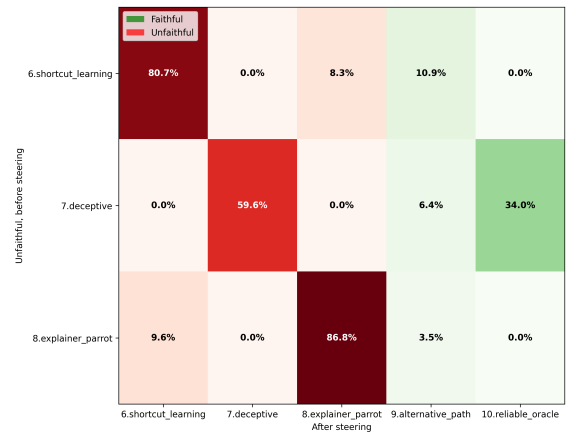


(b) Initially accurate predictions.

Figure 29: Detailed taxonomy transition state analysis, before and after hallucination inhibition on gemma-2-27b on 2-hop reasoning.



(a) Initially inaccurate predictions.



(b) Initially accurate predictions.

Figure 30: Detailed taxonomy transition state analysis, before and after NeuroFaith linear faithfulness steering on gemma-2-27b on 2-hop reasoning.

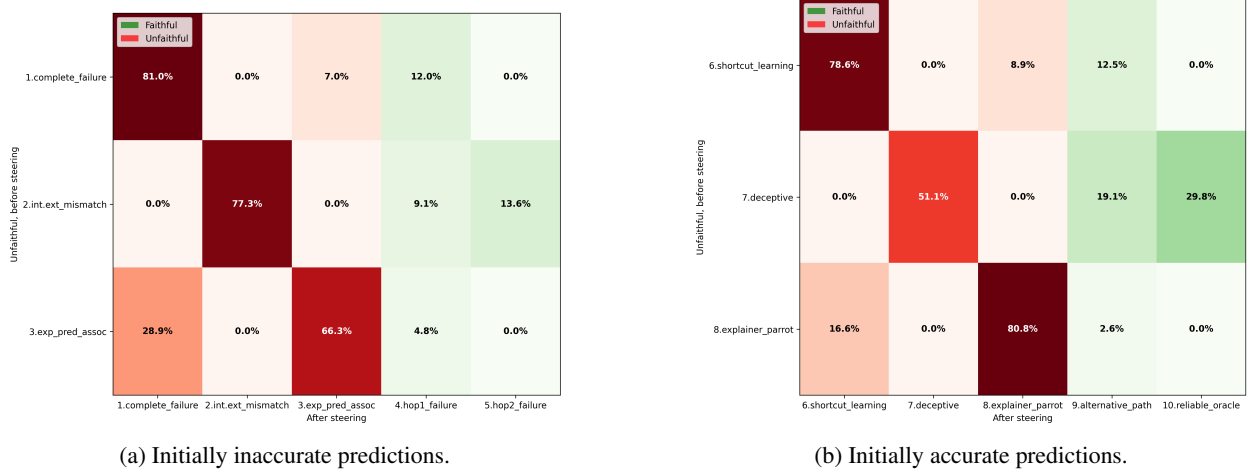


Figure 31: Detailed taxonomy transition state analysis, before and after hallucination inhibition on gemma-2-2b on 2-hop reasoning.

## F NeuroFaith Faithfulness Measure Comparison

In this section we examine how faithfulness as measured by NeuroFaith compares to existing Counterfactual Intervention (CI) Atanasova et al. (2023) and Attribution Agreement (AA) approaches Parcalabescu & Frank (2024) for evaluating LLM self-NLE faithfulness. We focus on 2-hop reasoning and begin with a qualitative comparison that illustrates potential differences between these approaches, followed by a quantitative analysis that provides evidence for these observations.

### F.1 2-hop Reasoning Faithfulness Qualitative Comparison.

To illustrate the critical differences between existing faithfulness evaluation approaches and NeuroFaith, we examine a concrete 2-hop reasoning example (see Figure 32) that illustrates fundamental limitations in current methods (CI and AA). Given input text  $x$ , prediction  $f(x)$ , and self-generated explanation  $e(x)$ , we compare how different faithfulness approaches evaluate the same case. The Example Setup:

- Original input:  $x = \text{"The father of Carol Chomsky is"}$
- Original prediction:  $f(x) = \text{"Harry Abraham Schatz"}$
- Counterfactual Intervention:  $x_{cf} = \text{"The father of the spouse of Carol Chomsky is"}$
- Counterfactual prediction:  $f(x_{cf}) = \text{"William Chomsky"}$

Counterfactual Intervention (CI) would assess the self-NLE  $e(x_{cf})$  as faithful. This evaluation is based solely on the presence of the intervention term "spouse" within  $e(x_{cf})$ , establishing consistency between the input modification and explanation content. Moreover, Attribution Analysis (AA) methods consists in comparing attribution scores (e.g., using SHAP) to highlight important tokens (e.g. "father", "spouse", "Carol", "Chomsky") for the prediction and the self-NLE. High correlation coefficients between the attribution vectors for prediction and self-NLE would similarly classify the self-NLE as faithful.

However, NeuroFaith rejects  $e(x_{cf})$  as unfaithful because the bridge object ("Morris Halle") is not contained in the decoded hidden states ( $\{\tilde{h}_k^\ell\}$ ). This mismatch between internal computation and self-NLE content reveals unfaithfulness. The steered self-NLE obtained with linear faithful steering (see Section 6) is evaluated as faithful by NeuroFaith, due to shared bridge object ("Noam Chomsky") between the new self-NLE and the decoded hidden states.

This qualitative example illustrates that both CI and AA approaches may employ more lenient evaluation standards compared to NeuroFaith and can miss unfaithful self-NLE. This observation is corroborated by our analysis in the next paragraph.

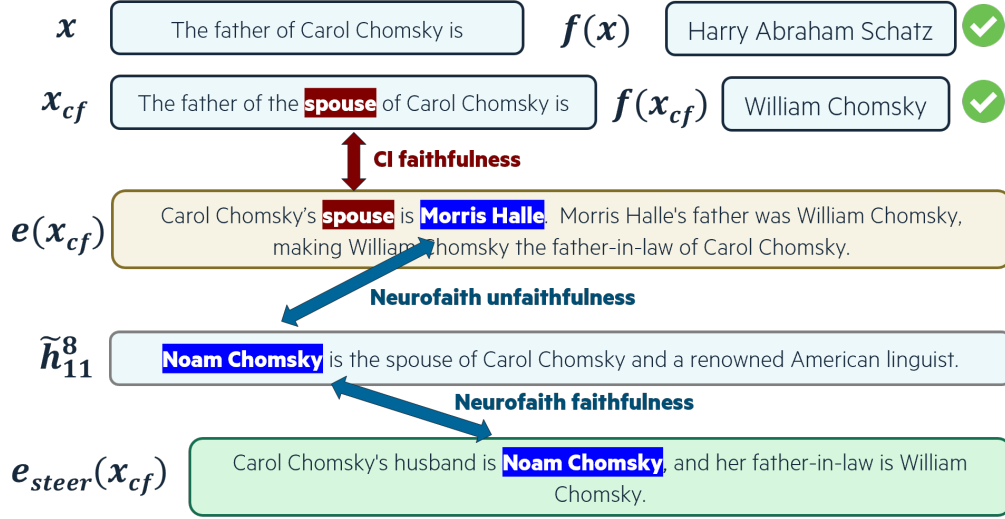


Figure 32: Qualitative comparison between NeuroFaith and CI faithfulness.

## F.2 2-hop Reasoning Faithfulness Quantitative Comparison.

We propose an experimental protocol to evaluate the practical utility of different faithfulness measures for model analysis. The protocol is motivated by two common applications of explanations in AI systems: (1) troubleshooting models by identifying the source of errors in wrong predictions Biecek & Samek (2024), and (2) detecting potential biases or shortcuts in correct predictions to ensure they align with expected reasoning processes Ribeiro et al. (2016).

We test whether faithful explanations, as identified by NeuroFaith and CI methods, provide better diagnostic information for these purposes. The key hypothesis is that if a faithfulness measure accurately captures the model’s internal reasoning, then explanations deemed faithful should better localize reasoning failures and identify non-canonical reasoning pathways.

**Experimental Framework.** Given an input text  $x = (o_1, r_1, \blacktriangle, r_2, \bullet)$  requiring 2-hop reasoning and the model’s reasoning trace  $(o_1, r_1, \hat{o}_2, r_2, \hat{o}_3)$ , we categorize model behavior using a simplified taxonomy (see Figure 33) based on prediction correctness and bridge object accuracy:

- Category A: Wrong prediction ( $\hat{o}_3 \neq o_3$ ), wrong bridge object ( $\hat{o}_2 \neq o_2$ ) → likely first-hop failure
- Category B: Wrong prediction ( $\hat{o}_3 \neq o_3$ ), correct bridge object ( $\hat{o}_2 = o_2$ ) → likely second-hop failure
- Category C: Correct prediction ( $\hat{o}_3 = o_3$ ), wrong bridge object ( $\hat{o}_2 \neq o_2$ ) → alternative reasoning pathway
- Category D: Correct prediction ( $\hat{o}_3 = o_3$ ), correct bridge object ( $\hat{o}_2 = o_2$ ) → canonical reasoning

Each category can be further subdivided with respect to faithfulness, enabling comparison between faithful and unfaithful self-NLE within each reasoning pattern. In the following we propose 3 metrics based on these 4 categories and assess if faithful self-NLE lead to better model debugging and bias targeting than unfaithful self-NLE.

**First Hop Hint.** We test whether faithful self-NLE better identify first-hop reasoning failures through a targeted intervention. For each input  $x$  having led to a wrong prediction ( $\hat{o}_3 \neq o_3$ ), we create a modified version  $x_{hint1} = (o_1, r_1, o_2, x)$  that explicitly provides the correct bridge object. For example:

- $x =$  "The country of origin of the movie maker that directed Persona is"
- $x_{hint1} =$  "The movie maker that directed Persona is Ingmar Bergman. The country of origin of the movie maker that directed Persona is"

If faithful self-NLE accurately reflect internal reasoning, then providing first-hop hints should differentially improve performance for Category A (first-hop failures) versus Category B (second-hop failures), and this difference should be stronger for faithful self-NLE. We define the performance ratio under first-hop hints as:

$$PR(A, B, hint1) = \frac{ACC(A, hint1)}{ACC(B, hint1)} \quad (3)$$

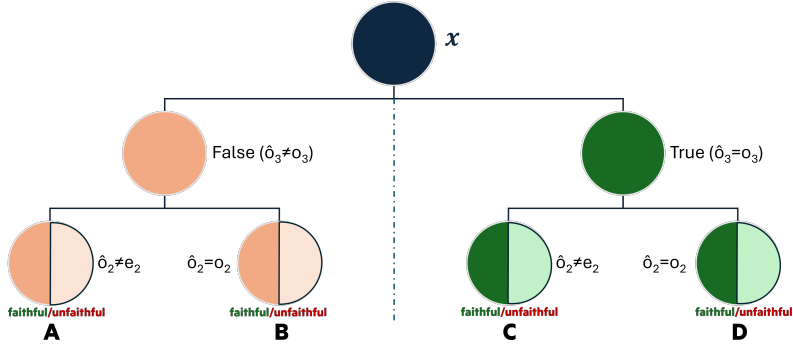


Figure 33: Simplified taxonomy of  $f$  behavior in two-hop reasoning, based on the status of the prediction and the self-NLE.

where  $ACC(A, hint1)$  represents the accuracy of Category A examples when given first-hop hints. We compute separate ratios for faithful and unfaithful explanations:

$$PR(A, B, hint1, faithful) = \frac{ACC(A, hint1, faithful)}{ACC(B, hint1, faithful)} \quad (4)$$

Finally, the Compound Accuracy Score (CAS) quantifies whether faithful explanations provide better error localization:

$$CAS(A, B, hint1) = \log\left(\frac{PR(A, B, hint1, faithful)}{PR(A, B, hint1, unfaithful)}\right) \quad (5)$$

A positive CAS indicates that faithful self-NLE better identify first-hop failures.

Quality Metric	gemma-2-2b		gemma-2-9b		gemma-2-27b	
	NeuroFaith	CI	NeuroFaith	CI	NeuroFaith	CI
hint1	<b>0.04</b>	-0.07	<b>0.06</b>	-1.10	<b>0.75</b>	-0.99
hint2	<b>-0.44</b>	-0.55	<b>0.28</b>	-0.03	-0.35	<b>1.25</b>
$r_2 \rightarrow r'_2$	<b>0.09</b>	-2.62	<b>0.17</b>	-0.32	<b>0.31</b>	-0.26

Table 12: NeuroFaith comparison to CI (higher is better) across models on 352 CI-compatible samples on 2-hop reasoning.

Quality Metric	gemma-2-2b	gemma-2-9b	gemma-2-27b
hint1	0.48	0.14	0.22
hint2	0.03	0.33	0.88
$r_2 \rightarrow r'_2$	-0.04	1.18	0.40

Table 13: NeuroFaith evaluation across models on the overall 2-hop reasoning dataset.

Table 14: Correlation analysis between NeuroFaith and CI.

**Second Hop Hint.** We now test whether faithful self-NLE better identify second-hop reasoning failures through a targeted intervention. Following the logic introduced above, for each input  $x$  having led to a wrong prediction ( $\hat{o}_3 \neq o_3$ ), we create a modified version  $x_{hint2} = (o_2, r_2, o_3, x)$  that explicitly provides the second part of the 2-hop reasoning. For example:

- $x =$  "The country of origin of the movie maker that directed Persona is"
- $x_{hint2} =$  "The country of origin of Ingmar Bergman is Sweden. The country of origin of the movie maker that directed Persona is"

If faithful self-NLE accurately reflect internal reasoning, then providing second-hop hints should differentially improve performance for Category B (second-hop failures) versus Category A (first-hop failures), and this difference should be stronger for faithful self-NLE. We build our second metric following the notations introduced above, based on the Compound Accuracy Score:

$$CAS(B, A, hint2) = \log\left(\frac{PR(B, A, hint2, faithful)}{PR(B, A, hint2, unfaithful)}\right) \quad (6)$$

Here, a positive CAS indicates that faithful self-NLE better identify second-hop failures.

**Second Relation Modification.** We test whether faithful self-NLE better identify non-canonical reasoning pathways through the modification of the second step of the reasoning trace ( $r_2$ ). Intuitively, a non-canonical reasoning pathways is more prone to lead to false reasoning when changing one step of the 2-hop reasoning. For each input  $x$  having led to a good prediction ( $\hat{o}_3 = o_3$ ), we create a modified version  $x_{r_2 \rightarrow r'_2} = (o_1, r_1, \blacktriangle, r'_2, \bullet)$  that change the second relation of the 2-hop reasoning input. For example:

- $x =$  "The country of origin of the movie maker that directed Persona is"
- $x_{r_2 \rightarrow r'_2} =$  "The father of the movie maker that directed Persona is"

If faithful self-NLE accurately reflect internal reasoning, then changing  $r_2$  should differentially decrease performance for Category C (alternative reasoning pathway) versus Category D (canonical reasoning), and this difference should be stronger for faithful self-NLE. We build our third metric following the notations introduced above, based on the Compound Accuracy Score:

$$CAS(D, C, r_2 \rightarrow r'_2) = \log\left(\frac{PR(D, C, r_2 \rightarrow r'_2, faithful)}{PR(D, C, r_2 \rightarrow r'_2, unfaithful)}\right) \quad (7)$$

A positive CAS indicates that faithful self-NLE better identify non-canonical reasoning pathways.

**Experimental Results.** We evaluate our three faithfulness indicators using both `NeuroFaith` and Counterfactual Intervention (CI). The Wikidata-2-hop dataset provides natural support for computing  $x_{r_2 \rightarrow r'_2}$  instances, as it contains multiple reasoning chains involving similar objects. Additionally, the dataset includes counterfactual interventions through variations in reasoning chains, enabling straightforward CI computation across multiple instances.

Our evaluation reveals three key findings. First, Table 12 shows that `NeuroFaith` consistently outperforms CI on the subset of CI-compatible samples. Second, Table 13 presents `NeuroFaith` results on the complete dataset, showing positive metric values across all models except `gemma-2-2b`.

## G Classification Examples

In this section we give two examples of instances characterized as either faithful or unfaithful in classification case.

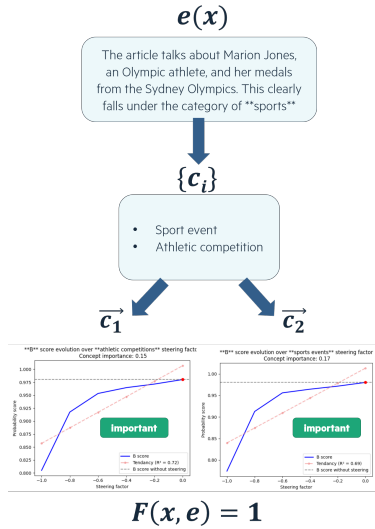


Figure 34: Example from the AGNews dataset where we detect "sport event" and "athletic competition" as relevant concepts from the explanation. These two concepts are assessed as important for the prediction, making this explanation faithful ( $F(x, e) = 1$ ).

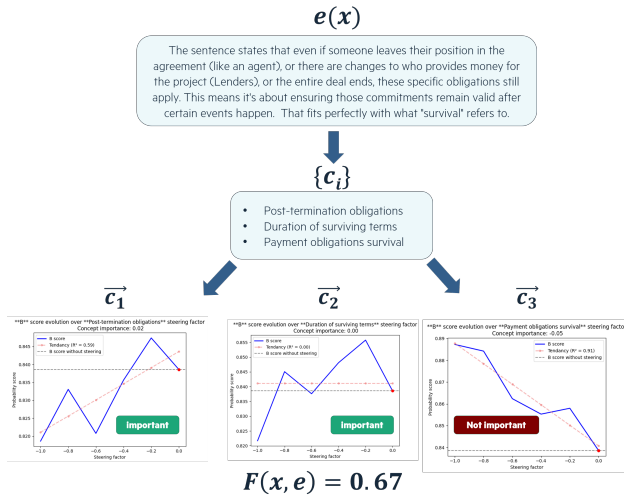


Figure 35: Example from the Ledger dataset where we detect "post-termination obligations", "duration of surviving terms" and "payment obligations survival" as relevant concepts from the explanation. Two concepts over three are assessed as important, giving an explanation faithfulness score at 0.67.

## H 2-hop Reasoning Taxonomy Examples

In this section we give examples of characterized instances based on the taxonomy introduced in Appendix E. We also give examples of unfaithful self-NLE made faithful, characterized by the same taxonomy.



Figure 36: Example from the Wikidata-2-hop dataset where we observe an internal-external reasoning mismatch. The model incorrectly answers "Jobete Music" and provides a self-NLE referencing to the bridge object "Sam Cooke". This bridge object is false and does not appear in the set of natural language interpretations of  $f$  latent states. However, the ground truth bridge object "Louis Armstrong" is decoded at token index 11 and layers 13 and 14.

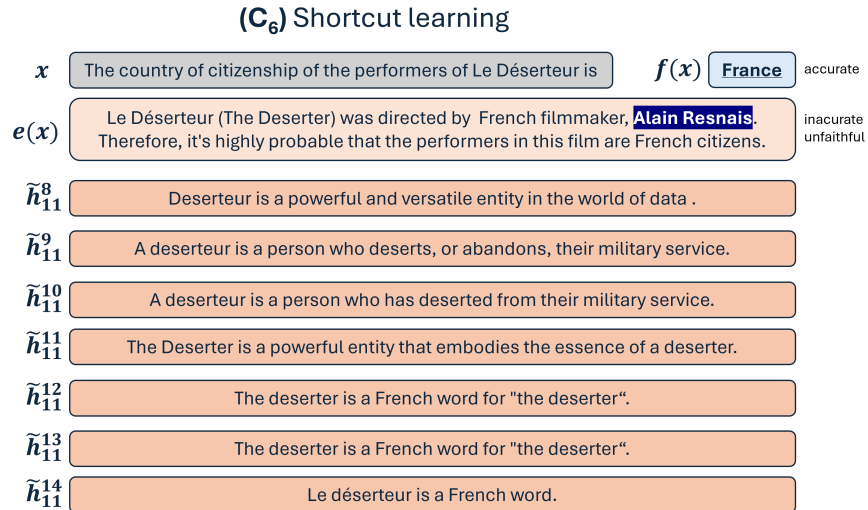


Figure 37: Example from the Wikidata-2-hop dataset where we observe shortcut learning. The model correctly answers "France" and provides a self-NLE referencing to "Alain Resnais". This bridge object is incorrect and does not appear in the set of natural language interpretations of  $f$  latent states.

(C<sub>7</sub>) Deceptiveness or hallucination

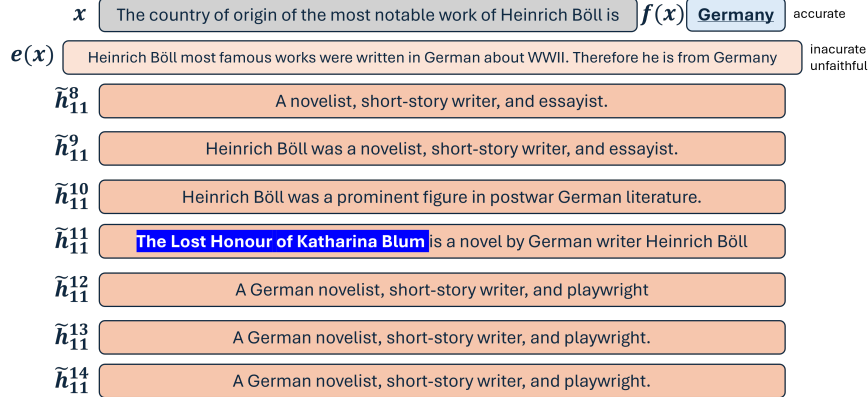


Figure 38: Example from the Wikidata-2-hop dataset where we observe shortcut learning. The model correctly answers "Germany" without providing any bridge object in its self-NLE. The expected bridge object "The Lost Honour of Katharina Blum" is however decoded from the representation space.

(C<sub>8</sub>) Explainer parrot

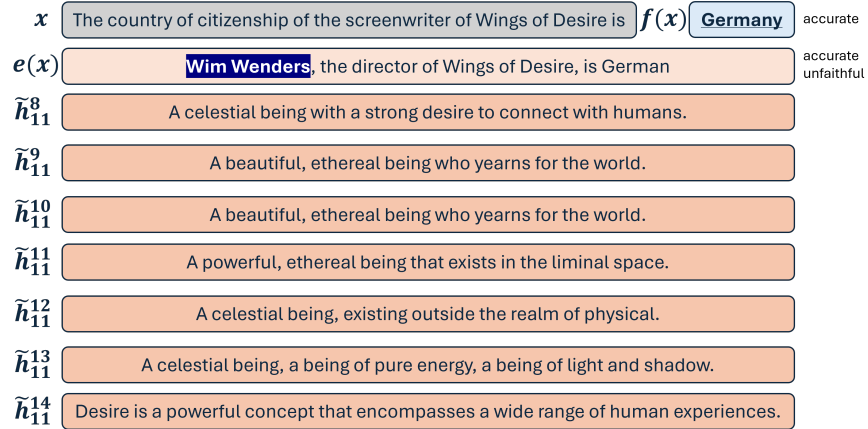


Figure 39: Example from the Wikidata-2-hop dataset where we observe an explainer parrot case. The model correctly answers "Germany" and provides a self-NLE referencing to "Wim Wenders". This bridge object is correct but does not appear in the set of natural language interpretations of  $f$  latent states.

(C<sub>9</sub>) Alternative reasoning pathway

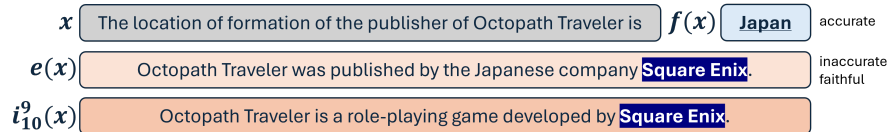


Figure 40: Example from the Wikidata-2-hop dataset where we observe an alternative reasoning pathway. The model correctly answers "Japan" and provides a self-NLE referencing to "Square Enix". This bridge object is incorrect and also appears in the set of natural language interpretations of  $f$  latent states.

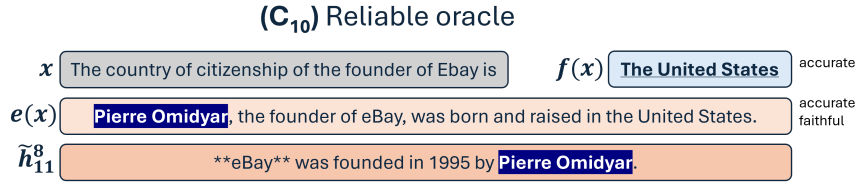


Figure 41: Example from the Wikidata-2-hop dataset where we observe an alternative reasoning pathway. The model correctly answers "USA" and provides a self-NLE referencing to "Pierre Omidyar". This bridge object is correct and also appears in the set of natural language interpretations of  $f$  latent states.

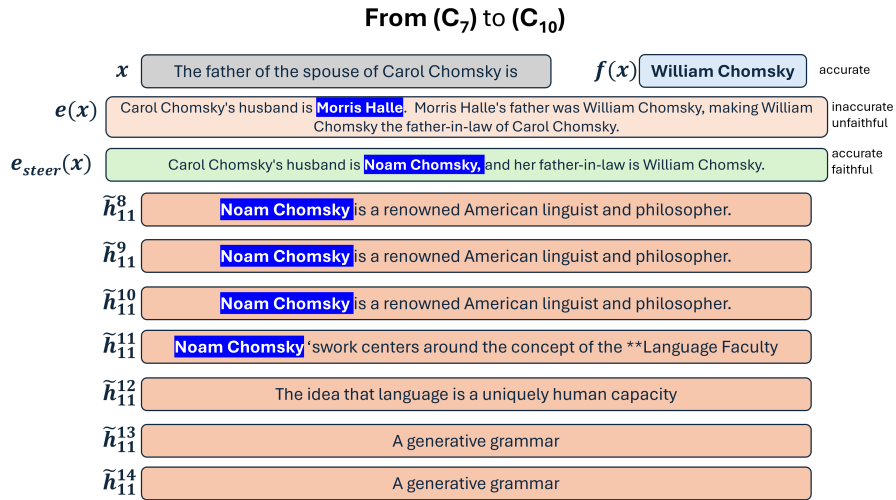


Figure 42: Example from the Wikidata-2-hop dataset where we start from an incorrect unfaithful explanation and go to a correct and faithful explanation through NeuroFaith linear faithfulness steering.

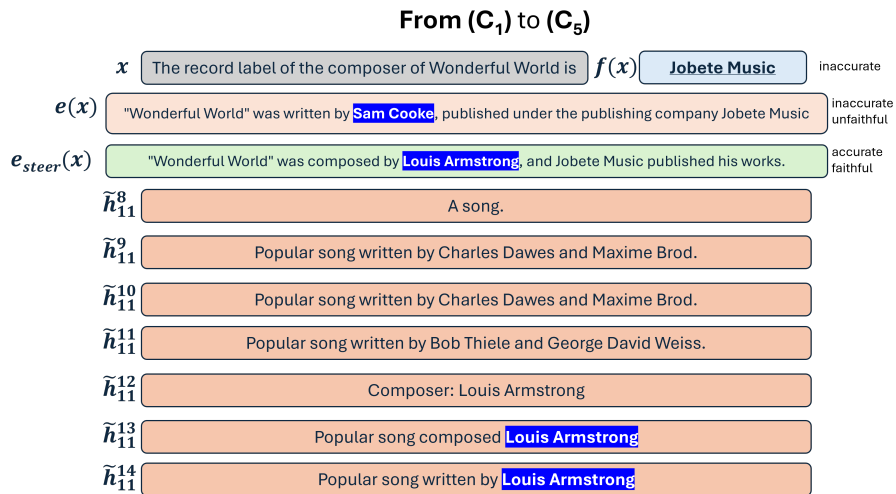


Figure 43: Example from the Wikidata-2-hop dataset where we start from an incorrect unfaithful explanation and go to a correct and faithful explanation through NeuroFaith linear faithfulness steering.



Figure 44: Example from the Wikidata-2-hop dataset where we start from an incorrect unfaithful explanation and go to a still incorrect but faithful explanation through NeuroFaith linear faithfulness steering.